

Discovery of Raltegravir, a Potent, Selective Orally Bioavailable HIV-Integrase Inhibitor for the Treatment of HIV-AIDS Infection

Vincenzo Summa,^{*†} Alessia Petrocchi,[†] Fabio Bonelli,[†] Benedetta Crescenzi,[†] Monica Donghi,[†] Marco Ferrara,[†] Fabrizio Fiore,[†] Cristina Gardelli,[†] Odalys Gonzalez Paz,[†] Daria J. Hazuda,[‡] Philip Jones,[†] Olaf Kinzel,[†] Ralph Laufer,[†] Edith Monteagudo,[†] Ester Muraglia,[†] Emanuela Nizi,[†] Federica Orvieto,[†] Paola Pace,[†] Giovanna Pescatore,[†] Rita Scarpelli,[†] Kara Stillmock,[‡] Marc V. Witmer,[‡] and Michael Rowley[†]

Istituto Di Ricerche Di Biologia Molecolare, P. Angeletti SpA (Merck Research Laboratories, Rome), Via Pontina Km 30, 600, 00040 Pomezia, Italy, Department of Antiviral Research, Merck Research Laboratories, West Point, Pennsylvania

Received March 6, 2008

Human immunodeficiency virus type-1 (HIV-1) integrase is one of the three virally encoded enzymes required for replication and therefore a rational target for chemotherapeutic intervention in the treatment of HIV-1 infection. We report here the discovery of Raltegravir, the first HIV-integrase inhibitor approved by FDA for the treatment of HIV infection. It derives from the evolution of 5,6-dihydroxypyrimidine-4-carboxamides and *N*-methyl-4-hydroxypyrimidone-carboxamides, which exhibited potent inhibition of the HIV-integrase catalyzed strand transfer process. Structural modifications on these molecules were made in order to maximize potency as HIV-integrase inhibitors against the wild type virus, a selection of mutants, and optimize the selectivity, pharmacokinetic, and metabolic profiles in preclinical species. The good profile of Raltegravir has enabled its progression toward the end of phase III clinical trials for the treatment of HIV-1 infection and culminated with the FDA approval as the first HIV-integrase inhibitor for the treatment of HIV-1 infection.

Introduction

Human immunodeficiency virus type 1 (HIV-1) is the causative agent of acquired immunodeficiency syndrome (AIDS). Despite decades of research and the successful development of combination therapies known as highly active antiretroviral therapy (HAART),^a HIV-1 remains one of the most serious health problems in the world. It is estimated that approximately 39 million people are living with HIV/AIDS worldwide, with infection and death rates of around 4 million and 3 million per year, respectively.¹ Currently, 22 drugs are approved by the FDA for the treatment of HIV infection. These are categorized according to their mode of action into four main groups: (i) the nucleoside reverse transcriptase inhibitors (NRTI), (ii) the non-nucleoside reverse transcriptase inhibitors (NNRTI), (iii) the protease inhibitors (PI), and (iv) entry inhibitors. Multidrug cocktails consisting of a protease inhibitor or a non-nucleoside reverse transcriptase inhibitor in combination with two nucleoside reverse transcriptase inhibitors is the current standard for HIV therapy (HAART). While HAART is undeniably effective, it can fail to control HIV replication in patients due to several limitations such as lack of therapy adherence, occurrence of side effects significantly affecting quality of life, and most importantly, the loss of drug effectiveness over time caused by development of resistance, including multidrug resistance and cross-resistance. It is therefore essential to continue to develop new antiretroviral drugs with potency against an ever-wider range of viral mutants including those which engender resistance to multidrug classes. Recently, viral entry inhibitors have been

pursued as novel anti-HIV agents: Enfuvirtide,² an injectable, peptidic anti-HIV drug blocking gp-41-mediated fusion, was licensed in 2003, and Maraviroc,³ which has recently been approved. Although over the years a plethora of HIV-1 integrase inhibitors have been discovered,⁴ Raltegravir is the first drug with this mechanism of action to be approved by FDA.

Proof-of-concept for the mechanism was first shown in an experimental model of retroviral infection using rhesus macaques infected with SHIV-89.6P with 8-hydroxy[1,6]-naphthyridine carboxamides.⁵ The robust antiviral activity in this model supplied evidence of in vivo efficacy for integrase inhibitors in retroviral infections, thereby establishing a solid base for the treatment of HIV-1 infection.⁶ Furthermore, proof-of-concept has also been achieved in man.⁷

HIV-1 integrase catalyzes the insertion of the viral DNA into the cellular genome of the host cell through a multistep process that includes two catalytic reactions: 3' endonucleolytic processing of the viral DNA ends and strand transfer, i.e., joining of the viral and cellular DNAs.⁸ Strand transfer is temporally and spatially separated from 3' processing and occurs after transport of the preintegration complex from the cytoplasm into the nucleus. Divalent metals, such as Mg²⁺, are required for not only 3' processing and strand transfer but also assembly of integrase onto specific viral donor DNA to form a complex competent to carry out either function. The architecture of the amino acids within the catalytic site and the geometry of the catalytic metals are highly conserved among a superfamily of nucleases and polynucleotidyl transferases, including also the NS5b RNA-dependent RNA polymerase of HCV virus. 4-Aryl-2,4-diketobutanoic acids (DKAs) were the first class of true HIV-1 strand transfer inhibitors and provided the first proof-of-concept for HIV-integrase inhibitors as antiviral agents in the cell based assay.⁹ DKAs were also discovered as active site HCV NS5b RNA-dependent RNA polymerase inhibitors.¹⁰ The mechanism of action of these inhibitors is likely a consequence of the interaction with metals in the active site, resulting in a functional impairment by chelation of the critical metal cofac-

* To whom correspondence should be addressed. Phone: +39 0691093680. Fax: +39 06 91093654. E-mail: vincenzo_summa@merck.com.

† Istituto Di Ricerche Di Biologia Molecolare, P. Angeletti SpA (Merck Research Laboratories, Rome).

[‡] Department of Antiviral Research, Merck Research Laboratories.

^a Abbreviations: FDA, Food and Drug Administration; HAART, highly active antiretroviral therapy; NRTI, nucleoside reverse transcriptase inhibitor; NNRTI, Non-nucleoside reverse transcriptase inhibitor; PI, protease inhibitor; DKA, diketoacid; FBS, fetal bovine serum; NHS, normal human serum.

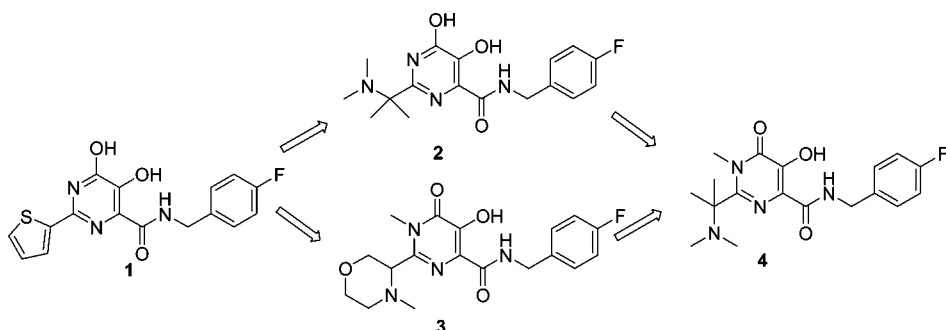


Figure 1. Optimization of dihydroxypyrimidine and *N*-methyl pyrimidinone carboxamides as HIV-integrase strand transfer inhibitors.

tors.¹¹ Within Merck Research Laboratories (MRL), the two groups working on HIV-integrase and HCV polymerase discovered a series of scaffolds characterized by improved drug-like qualities that dialed out the undesirable DKA properties. In particular, we discovered that the dihydroxypyrimidine carboxamide derived from the evolution of DKA in the HCV polymerase program¹² was a potent, reversible, and selective HIV-integrase strand transfer inhibitor showing nanomolar activity in the enzymatic assay ($IC_{50} = 0.085 \mu M$) while being completely inactive on the HCV polymerase.¹³ Extensive structure activity relationship studies on the carboxamide moiety led to the identification of the *p*-fluorobenzyl as the optimal amide residue¹⁴ (**1**, Figure 1) and of the *gem*-dimethyl as the optimal 2-substituent for the dihydroxypyrimidine core¹⁵ (**2**). Parallel efforts led to the identification of the related *N*-methylpyrimidone scaffold showing equal or enhanced activity for the HIV-integrase (**3**). Both **2** and **3** showed good potency in the antiviral cell based assay in the presence of 50% normal human serum (NHS) and favorable oral bioavailability in preclinical species.¹⁶

Raltegravir (**27**) is the result of our continued efforts to optimize these inhibitors, addressing issues presented by previously reported inhibitors. These include metabolic stability, pharmacokinetic profile, antiviral activity against a panel of HIV-1 integrase mutations previously shown to be associated with resistance to 1,3-diketoacid inhibitors and other classes of inhibitors, and genotoxicity. The antiviral properties and pre-clinical pharmacological profile of Raltegravir are described here: these qualities have enabled its progression toward the end of phase III clinical trials for the treatment of HIV-1 infection and AIDS, positioning it as the first HIV-integrase inhibitor approved by FDA for the treatment of HIV-1 infection.¹⁷

Results and Discussion

As part of our continued effort to optimize the two classes of inhibitors represented by **2** ($IC_{50} 0.05 \mu M$; $CIC_{95} 0.06 \mu M$ 10% FBS; $CIC_{95} 0.078 \mu M$ 50% NHS) and **3** ($IC_{50} 0.06 \mu M$; $CIC_{95} 0.06 \mu M$ 10% FBS; $CIC_{95} 0.10 \mu M$ 50% NHS), we combined the optimal properties of each series in a single molecule in order to capitalize on the different physicochemical properties of the scaffolds. The straightforward modification was to convert the dihydroxypyrimidine derivative **2**¹⁵ into the corresponding *N*-methyl pyrimidinone **4** (Figure 1). The modification did not lead to the desired result, as the compound was less potent both in the enzymatic and cell based assays (Table 1). Initial structure activity relationship studies were conducted in order to improve the activity against integrase, focusing in particular on the basic amine and the *gem*-dimethyl moieties of inhibitor **4**. This effort led to compounds such as morpholine **5** and tetrahydropyran **6**, both showing low nanomolar activity

in the enzymatic assay (**5** $IC_{50} = 0.003 \mu M$; **6** $IC_{50} = 0.002 \mu M$) and good potency in the antiviral cell based assays in low serum condition (**5** $CIC_{95} = 0.065 \mu M$; **6** $CIC_{95} = 0.250 \mu M$ 10% FBS). However, a large potency shift was observed in the presence of 50% NHS for both analogues, which led us to explore other modifications. The simple acetamide derivative **7** showed a good potency in all assays and limited shift in high serum conditions. Various acetamide replacements such as sulfonamide **8**, urea **9**, and sulfamide **10** were also prepared. While for all these analogues the potency in the enzyme assay was in the nanomolar range ($IC_{50} = 0.007$ – $0.018 \mu M$), in the antiviral cell based assay, the compounds showed a larger variability in the activity values, ranging from 0.062 to $>1.0 \mu M$ in low serum conditions. Only **7** and **10** retained activity below 1 μM in high serum conditions ($CIC_{95} = 0.4$ and 0.5 μM 50% NHS for **7** and **10**, respectively).

The amide functionality offered the opportunity to explore very rapidly a large series of fragments by rapid analogue synthesis. We discovered that the introduction of an oxalamide moiety on the scaffold resulted in a very potent compound both in the enzymatic and antiviral cell based assays (Table 2):¹⁸ compound **11** showed an $IC_{50} = 0.010 \mu M$ on the enzyme and a marginal shift in the cell based assay, having $CIC_{95} = 0.045$ and $0.074 \mu M$ in 10% FBS and 50% NHS, respectively. The corresponding ester **12** and acid **13** showed the same level of potency on the enzyme but were significantly less potent in the cell based assays. Methylation of the oxalamide NH was detrimental: compound **14** showed both decreased enzymatic potency and activity in the cell based assay compared to **11** ($IC_{50} = 0.015 \mu M$; $CIC_{95} = 0.062$, $0.125 \mu M$ 10% FBS and 50% NHS, respectively). A number of analogues were prepared to explore replacement of the *N,N*-dimethyl fragment of the oxalamide moiety. Among those, two of the most relevant examples are the morpholine derivative **15** and the *N*-methyl piperazine derivative **16**, both of which showed good levels of potency. However, the *N,N*-dimethyloxalamide substituent remained the most potent substituent within this series.

The benzylamide moiety of **11** was also revisited with a selection of amides known from previous work on the project to modulate the physicochemical properties of our inhibitors.¹³ In particular, it was observed that the protein binding was influenced by the substituent present on the aromatic ring. The *N*-Me carboxamide (**17**, Table 3) had low activity on the enzyme, reinforcing the importance of the benzyl amide as key fragment for enzymatic activity. Introduction of more polar substituents with respect to 4-F on the phenyl ring of the benzylamides were generally tolerated in terms of enzymatic potency, while the 2,3-dimethoxy derivative **18** was found to be a weak inhibitor in the cellular based assay, the 2-methylsulfone-4-fluoro **19** showed high activity with no shift between low and high serum conditions. The more lipophilic benzylamide

Table 1. 2-Substituted-*N*-methyl Pyrimidone Derivatives

Cpd	R ₁	R ₂	Inhibition of Strand Transfer IC ₅₀ (μM) ^a	10% FBS Antiviral Activity CIC ₉₅ (μM) ^b	50% NHS Antiviral Activity CIC ₉₅ (μM) ^b
4		Me	0.230	1.00	>1.00
5		Me	0.003	0.065	0.50
6			0.002	0.250	1.00
7		Me, Me	0.007	0.310	0.40
8		Me, Me	0.008	0.062	1.00
9		Me, Me	0.018	1.00	>1.00
10		Me, Me	0.012	0.125	0.50

^a Assays were performed with recombinant HIV-1 integrase (0.01 μM) preassembled on immobilized oligonucleotides. Inhibitors were added after assembly and washings, and IC₅₀ is the concentration of inhibitor that reduces HIV-integrase activity by 50%. Results are the mean of at least 3 independent experiments; SD was always ± 8% of the value. ^b Spread assay: 95% cell culture inhibitory concentrations for inhibition of the spread of HIV-1 infection in cell culture, using HIV-1IIb and MT-4 T-lymphoid cells, in a medium containing 10% heat-inactivated fetal bovine serum or 50% normal human serum. Results are the mean of at least 3 independent experiments, SD was always < ±10% of the value. For details see ref 10.

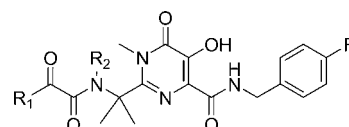
analogue **20** proved to be a potent inhibitor in the cellular assay in low serum conditions, although a 4-fold shift in activity was observed in 50% NHS (IC₅₀ = 0.009 μM; CIC₉₅ = 0.031 μM 10% FBS; CIC₉₅ = 0.130 μM 50% NHS). Overall, these results highlighted that the 4-fluorobenzylamide remains the optimal substituent even within an optimized scaffold such as the one of analogue **11**.

Next, we moved to investigate aromatic and heteroaromatic amides as capping groups of the amine portion of the scaffold **11** (Table 4). While the aromatic derivatives showed modest potency in the antiviral cell based assay (data not shown), the heteroaromatic ones proved to be very active. The original fragment screening was conducted with the idea to have heteroatoms in the same positions where the heteroatoms of the oxalamide are located. The simple 2-pyridine carboxamide **21** showed low nanomolar activity on the enzyme, a 6-fold shift in the spread assay in low serum, but reduced activity in high serum (IC₅₀ = 0.02 μM; CIC₉₅ = 0.125 μM 10% FBS; CIC₉₅ = 1.00 μM 50% NHS). The other pyridine isomers were less potent in the cell based assay (data not shown). The introduction of a second nitrogen in the ring led to the more polar pyridazine derivative **22**, which showed a reduced shift in potency between the low and high serum conditions (CIC₉₅ = 0.062 μM 10% FBS; CIC₉₅ = 0.50 μM 50% NHS). The isomeric pyrimidine derivative **23** was potent in all assays (IC₅₀ = 0.007 μM; CIC₉₅ = 0.02 μM 10% FBS; CIC₉₅ = 0.050 μM 50% NHS). Five-

membered ring heterocycles were also investigated in depth, and compounds bearing two or three heteroatoms were the most potent in the cell based assays, with heterocycles having a heteroatom in the 2-position being the most active. Oxazole **24**, thiazole **25**, and imidazole **26** all showed single-digit nanomolar activity on the enzyme. In contrast, in the cellular antiviral assay, they showed different degrees of activity. Oxazole **24** had CIC₉₅ = 0.50 μM in both serum conditions, while thiazole **25** had higher activity in low serum and showed 4-fold shift in high serum and imidazole **26** showed the best activity in high serum conditions (CIC₉₅ = 0.250 μM 50% NHS). Among the heterocycles having three heteroatoms, oxadiazole **27** was the best, being one of the most potent compounds in the cell based assay (CIC₉₅ = 0.019 and 0.031 μM in 10% FBS and 50% NHS, respectively). Other heterocycles having a similar heteroatom arrangement, including the corresponding triazole **28**, showed a lower activity in the antiviral assay.

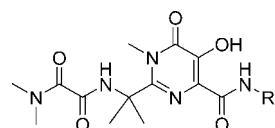
Selectivity, Drug Metabolism and Pharmacokinetics

The most potent compounds in the antiviral cellular assays were further profiled, and between them **11** and **27** were preferred over the others. **11** and **27** were tested and were found to be essentially inactive (IC₅₀'s > 50 μM) against a series of related enzymes such as HCV polymerase, HIV RT, HIV RNase-H, and human α-, β-, and γ-polymerases. This shows the high degree of selectivity for integrase over the other

Table 2. Oxalamide Derivatives

Cpd	R ₁	R ₂	Inhibition of Strand Transfer IC ₅₀ (μM) ^a	10% FBS Antiviral Activity CIC ₉₅ (μM) ^b	50% NHS Antiviral Activity CIC ₉₅ (μM) ^b
11		H	0.010	0.045	0.074
12		H	0.015	1.00	>1.00
13		H	0.004	0.250	1.00
14		Me	0.015	0.062	0.125
15		H	0.020	0.125	0.125
16		H	0.026	0.125	0.250

^a Assays were performed with recombinant HIV-1 integrase (0.01 μM) preassembled on immobilized oligonucleotides. Inhibitors were added after assembly and washings, and IC₅₀ is the concentration of inhibitor that reduces HIV-integrase activity by 50%. Results are the mean of at least 3 independent experiments; SD was always ± 8% of the value. ^b Spread assay: 95% cell culture inhibitory concentrations for inhibition of the spread of HIV-1 infection in cell culture, using HIV-1IIb and MT-4 T-lymphoid cells, in a medium containing 10% heat-inactivated fetal bovine serum or 50% normal human serum. Results are the mean of at least 3 independent experiments, SD was always < ±10% of the value. For details see ref 10.

Table 3. Benzylamide Moiety Derivatives

Cpd	R ₁	Inhibition of Strand Transfer IC ₅₀ (μM) ^a	10% FBS Antiviral Activity CIC ₉₅ (μM) ^b	50% NHS Antiviral Activity CIC ₉₅ (μM) ^b
11		0.010	0.045	0.074
17	Me	>5.000	>10.0	>10.0
18		0.021	1.0	>1.00
19		0.004	0.125	0.125
20		0.009	0.031	0.130

^a Assays were performed with recombinant HIV-1 integrase (0.01 μM) preassembled on immobilized oligonucleotides. Inhibitors were added after assembly and washings, and IC₅₀ is the concentration of inhibitor that reduces HIV-integrase activity by 50%. Results are the mean of at least 3 independent experiments; SD was always ± 8% of the value. ^b Spread assay: 95% cell culture inhibitory concentrations for inhibition of the spread of HIV-1 infection in cell culture, using HIV-1IIb and MT-4 T-lymphoid cells, in a medium containing 10% heat-inactivated fetal bovine serum or 50% normal human serum. Results are the mean of at least 3 independent experiments, SD was always < ±10% of the value. For details see ref 10.

enzymes that work through a Mg²⁺ catalyzed reaction. To assess the selectivity toward other unrelated targets with different mechanisms of action, the two agents were also tested in the Pan Laboratories screen having 150 enzymes, channels, and receptors, and they showed no significant activity <10 μM.

Neither of the two compounds inhibited any of the major Cytochrome P450 isoforms, with IC₅₀'s > 50 μM for 1A2, 2C9, 2D6, 3A4, and 2C9, nor showed time dependent inhibition of the 3A4 isoform. Both compounds had binding affinity >50 μM on hERG channels.

Table 4. Heteroaromatic Capping Group

Cpd	R ₁	Inhibition of Strand Transfer IC ₅₀ (μM) ^a	10% FBS Antiviral Activity CIC ₉₅ (μM) ^b	50% NHS Antiviral Activity CIC ₉₅ (μM) ^b
21		0.020	0.125	1.00
22		0.015	0.062	0.50
23		0.007	0.020	0.050
24		0.007	0.500	0.500
25		0.008	<0.078	0.312
26		0.006	0.250	0.250
27		0.015	0.019	0.031
28		0.004	0.250	1.00

^a Assays were performed with recombinant HIV-1 integrase (0.01 μM) preassembled on immobilized oligonucleotides. Inhibitors were added after assembly and washings, and IC₅₀ is the concentration of inhibitor that reduces HIV-integrase activity by 50%. Results are the mean of at least 3 independent experiments; SD was always ± 8% of the value. ^b Spread assay: 95% cell culture inhibitory concentrations for inhibition of the spread of HIV-1 infection in cell culture, using HIV-1IIb and MT-4 T-lymphoid cells, in a medium containing 10% heat-inactivated fetal bovine serum or 50% normal human serum. Results are the mean of at least 3 independent experiments, SD was always < ±10% of the value. For details see ref 10.

Table 5. iv Pharmacokinetic Parameters for Rats, Dogs, and Rhesus Monkeys for **11** and **27**

compd	species	Cl _p ^c (mL/min/kg)	αT _{1/2} ^d (h)	βT _{1/2} ^e (h)	V _d ^f (L/kg)	dose (mg/kg)
11	rat ^a	20	0.4	6	1.3	3
11	dog ^a	11	1.2	16	1.1	5
11	rhesus ^b	14	0.9	3	2.9	1
27	rat ^a	39	ND	2	2.0	3
27	dog ^a	6	ND	11	0.9	1
27	rhesus ^a	18	ND	4	1.2	1

^a Vehicle iv DMSO/saline 20%/80%. ^b Vehicle iv DMSO. ^c Plasma clearance. ^d Plasma primary phase half-life following iv administration. ^e Terminal plasma half-life following iv administration. ^f Volume of Distribution. ND Not done.

The pharmacokinetic profiles of **11** and **27** were determined in Sprague-Dawley rats, dogs, and rhesus monkeys. In rats, various formulations and salts were studied. Dosing **11** in rats at 3 mg/kg po using methyl cellulose as vehicle, the exposure and C_{max} were increased and T_{1/2} was prolonged using the sodium salt with respect to the free acid (Na⁺ salt AUC = 2.2 μM·h, C_{max} = 4.1 μM, T_{1/2} = 2.3 h; free OH AUC = 0.7 μM·h, C_{max} = 0.6 μM, T_{1/2} = 0.9 h; Table 6). Dose proportionality studies were performed using methyl cellulose as a vehicle for **11** as free OH dosed po at 1, 4, 15, 50 as solutions and 100 mg/kg as a suspension, where the AUC and C_{max} increased linearly (R² 0.95 and 0.94, respectively). Using PEG400 as vehicle at 100 mg/kg, the compound was completely soluble, and the exposure and the C_{max} increased 2.5-fold with respect

to the previous formulation (1% methyl cellulose AUC = 23 μM·h, C_{max} = 12 μM; PEG400 AUC = 49 μM·h, C_{max} = 31 μM). The same effect was observed dosing the compound in dogs at 10 mg/kg in 1% methyl cellulose, where the sodium salt gave higher exposure, C_{max}, and prolonged T_{1/2} compared to the free OH, (Na⁺ salt AUC = 47 μM·h, C_{max} = 32 μM, T_{1/2} = 11.9 h; free OH AUC = 23 μM·h, C_{max} = 11.1 μM, T_{1/2} = 4.9 h). No advantages were observed dosing the free OH in PEG400, as the exposure was similar to the Na⁺ salt in methylcellulose (AUC PEG400-MC Na⁺ salt = 44 vs 47 μM·h). **11** was also dosed po at 10 mg/kg in rhesus monkeys as free OH in 1% methyl cellulose: the exposure and plasma half-life were modest in comparison to the other preclinical species (AUC = 5.2 μM·h, C_{max} = 4.5 μM, T_{1/2} = 1.9 h), probably due to the low solubility in the conditions of the study. These findings led to the decision to use the Na⁺ salt as the optimal form for safety studies.

Values of plasma clearance (Cl_p), volume of distribution (V_{dss}), and plasma half-life (T_{1/2}) in rats, dogs, and rhesus monkeys were calculated dosing **11** iv; data are reported in Table 5. Considering the liver blood flow, clearance was moderate for all species with a rank order of rhesus, rat, and dog. The volume of distribution was modest for all species. Plasma half-life showed a multiphasic elimination, with a relatively short α-phase and a prolonged β-phase for all species.

Good oral bioavailability was observed in dog and rat dosing **11** as Na⁺ salt (F = 93 and 36% for dog and rat, respectively),

Table 6. Rat, Dog, and Rhesus Monkey po Pharmacokinetic Parameters for **11** and **27**

compd	<i>F</i> ^a (%) rat/dog/rhesus	<i>C</i> _{max} ^b (μ M) rat/dog/rhesus	po <i>t</i> _{1/2} ^c (h) rat/dog/rhesus	<i>AUC</i> ^d (μ M·h) _(mg/kg) rat/dog/rhesus	PPB ^e (% free) rat/dog/rhesus/human
11 Na ⁺	36/93/nd	4.1 ₍₃₎ /32 ₍₁₀₎ /nd	2.3/11.9/nd	2.2 ₍₃₎ /47 ₍₁₀₎ /nd	35/38/18/28
11 OH	nd/nd/24	0.6 ₍₃₎ /11 ₍₁₀₎ /4.5 ₍₁₀₎	0.9/4.9/1.9	0.7 ₍₃₎ /23 ₍₁₀₎ /5.2 ₍₁₀₎	
27 Na ⁺	nd/nd/nd	1.0/nd/nd	nd/nd/nd	1.4 ₍₃₎ /nd/nd	26/29/15/17
27 K ⁺	45/69–85/nd	1.6/4.6 ₍₂₎ –24 ₍₁₀₎ /nd	7.5/13/nd	1.3 ₍₃₎ /11 ₍₂₎ –45 ₍₁₀₎ /nd	
27 OH	37/45/8	1.2 ₍₃₎ /3 ₍₂₎ –8 ₍₁₀₎ /0.3	nd/nd/7	1.0 ₍₃₎ /7 ₍₂₎ –21 ₍₁₀₎ /1.8 ₍₁₀₎	

^a Oral bioavailability. ^b Maximum plasma concentration after po administration. ^c Terminal phase plasma half-life following po administration. ^d Area under the curve following po administration. ^e Plasma protein binding (free fraction). nd = not done.

while lower oral exposure was achieved in rat and rhesus dosing **11** as free OH, probably due to lower solubility and related incomplete absorption (*F* = 34 and 24% rat and rhesus, respectively). Plasma protein binding was measured for human and the three preclinical species: the free fraction was high for all species with a rank order rat, dog, human, and rhesus (35, 38, 28, and 18%, respectively, all data reported in Table 6).

The pharmacokinetic profile of **27** was also studied using different crystalline salts with 1% methyl cellulose as the vehicle of choice to conduct po dosing. This choice was based on the previous experience with **11**, where the PEG400 was equivalent or worse than the Na⁺ salt in 1% methyl cellulose. Furthermore, 1% methyl cellulose is one of the most frequently used vehicles to conduct safety studies in preclinical species. **27** was dosed in rat at 3 mg/kg using three different forms (free OH, Na⁺, and K⁺ salts), and higher exposures were achieved with the salts (AUC Na⁺ = 1.4, K⁺ = 1.3, free OH 1.0 μ M·h, respectively). Dose proportionality studies using 1, 4, 15, 60, 100 mg/kg were performed both on the crystalline free OH and the crystalline K⁺ salt. The first was less than dose proportional although the AUC increased (data not reported). Much better results were obtained with the crystalline K⁺ salt, with AUC increasing linearly and in a dose proportional manner (*R*² = 0.95, AUC from 0.8 to 35 μ M·h). In contrast, the *C*_{max} was less than dose proportional. In dog, **27** was dosed at 2 and 10 mg/kg as free OH and K⁺ salt, both crystalline. The AUCs and *C*_{max} were higher for the K⁺ salt at both doses (AUC 2 mg/kg = 7 vs 11; 10 mg/kg = 21 vs 45 μ M·h; *C*_{max} 2 mg/kg 3 vs 4.5, 10 mg/kg 8 vs 24 free OH vs K⁺, respectively). The terminal plasma half-life (*T*_{1/2}) after 10 mg/kg po of the K⁺ salt was 13 h. The crystalline free OH was dosed at 10 mg/kg in rhesus monkey showing a modest exposure and *C*_{max} (AUC = 1.8 μ M·h; *C*_{max} = 0.3 μ M). **27** was dosed iv using as vehicle 20% DMSO/40% Peg400/40% H₂O at 3 mg/kg in rat and 1 mg/kg in dog and rhesus. The corresponding plasma clearances (Cl_p) were 39, 6, and 18 mL/min/kg and volume of distribution (*V*_{ds}) 2.0, 0.9, and 1.2 L/kg for rat, dog, and rhesus, respectively. The oral bioavailabilities, calculated for the po experiments, were 45% in rat, 69–85% in dog dosing the crystalline K⁺ salt, and 37, 45, and 8% in rat, dog, and rhesus, respectively, with the crystalline free OH (Table 6).

The PK data conducted with different vehicles and salt forms indicated that the Na⁺ or K⁺ salt showed better po profile for the exposure and solubility properties, and these crystalline salt forms were therefore selected for further studies in safety assessment.

The plasma protein binding was measured for preclinical species and human, showing modest interspecies variability of the free fraction values (rat 26.6%, dog 29.1%, rhesus 15.4%, and human 17.2% free, Table 6).

The metabolism of the two agents was studied in liver microsomes of rat, dog, rhesus, and human. The compounds had the same route of metabolism previously reported for this class of molecules in that they were very stable in liver

microsomes in the presence of NADPH, showing that oxidative metabolism does not play a significant role. The major route of metabolism proved to be glucuronidation, with the rate of metabolism in the presence of UDPGA showing a clear rank order between species, (rhesus > rat > human > dog) with values equal to 46, 20, 8, and 3 μ L/min/kg for **11** and 36, 34, 9, and 2 for **27**. The same metabolism profile was observed in the presence of hepatocytes. The compounds did not react with glutathione after incubation at 37 °C for 24 h. [³H]-**11** and [³H]-**27** were used to measure the irreversible protein covalent binding in vivo (rat 25 mpk po) to liver, kidney, and plasma and in vitro to human and rat liver microsomes. In both assays, the covalent binding was <50 pmol-equivalent/mg-protein for both compounds. The in vivo metabolism was also investigated in rat using the radiolabeled material and in rat and dog by NMR. In rats, **11** was eliminated mainly by metabolism. Urinary and biliary secretion of intact drug amounted to 8% and 5% of the administered dose, respectively. In dogs, 13% of the dose was excreted unchanged in urine after po dosing. The major metabolite of **11** detected in rat urine and bile and dog urine was the 5-*O*-glucuronide conjugate. In rat and dog excreta, no other metabolites were detected by ¹⁹F-NMR: 90% of total fluorine signal accounts for the 5-*O*-glucuronide. Dosing **27** iv in rats a recovery of 50% of the dose in bile and 20% in urine (glucuronide plus parent compound) was observed. The amount of glucuronide in bile and urine after iv dosing was 90% of the total fluorine signal and the intact compound was 10%. Following oral dosing, around 20% of the dose was recovered in rat urine (glucuronide plus parent compound). In dogs, after iv dosing of **27**, around 30% of the dose was recovered in urine (0–24 h). The amount of intact compound in the urine was 65% of the total fluorine signal and the glucuronide was 35%. Following oral dosing the amount of **27** excreted in urine was 10% of the dose (glucuronide plus parent compound). The same profiles were found using the ³H-materials. These data were in perfect agreement with the microsome stability data, showing glucuronidation as the major route of metabolism. The glucuronide of **27** was fully characterized using ¹H, ¹³C, and ¹H–¹³C correlation NMR spectroscopy, which confirmed the formation of the glucuronide conjugate of the hydroxyl group in position 5 of the pyrimidinone ring. The full assignment of all ¹H and ¹³C signals ascribed to these β -glucuronides was achieved using the crude sample of urine after solid phase extraction.¹⁹

Comparing the in vivo and in vitro data, the human pharmacokinetic profile was predicted to be similar to the dog. Looking at the po profile, it was clear that both **11** and **27** showed biphasic elimination with a short α -phase and a prolonged β -phase. This behavior was a very important feature to maintain the plasma concentration well above the CIC₉₅ at 12 h (**11** Na⁺ salt CIC₉₅ = 125 nM 50% NHS; dog C₁₂ h 246 nM at 10 mg/kg; **27** K⁺ salt CIC₉₅ = 31nM 50% NHS; dog C₁₂ h 160 and 350 nM at 2 and 10 mg/kg, respectively). Taking into account the plasma protein binding, the metabolic stability

Table 7. Resistance Profiles with HIV-1 Containing Site-Directed Integrase Mutations^a

mutations	T66I	V151I	F121Y	T125K	T66I* ^b	M154I	T66I* ^b	S153Y	N155S* ^b	T125K* ^b	F121Y	T66I*/L74M ^b	V151I
L-870810	1	1	3	0.5	3		1.3		10	12		9	
11	3	1	12	1	5		8		40	19		35	
27	1	1	3	1	1		1		10	8		6	
S-1360	12	4	14	2	20		50		>50	50		100	

^a Shift in IC₅₀ relative to wild type HIV-1—single cycle infectivity assay. ^b * = Viruses that exhibit >50% reduction in specific infectivity.

(intrinsic clearance), and the plasma clearance for all species, the human dosing regimen was predicted to be BID.

The compounds were also evaluated in the Ames test and resulted negative both in the presence and in the absence of S9 fraction. This finding was in contrast to what had previously been observed for **3**, which proved positive in the same assay showing a reversion on the strain TA 1535 and was therefore not further developed.

11 and **27** shared very similar DMPK profiles, with **27** clearly being the more potent of the two in the antiviral assay in presence of high serum. We decided to include another parameter to discriminate between the two compounds. Considering how important it is to profile HIV drugs against mutants raised in the clinic and the correlation that they have with the mutants generated in cell culture, we decided to profile the two agents against a series of HIV-integrase mutants, which had been raised during the course of many years of research in our laboratories using different classes of inhibitors both from our research and coming from the work of other institutions or pharmaceutical companies (Table 7). The assay employed is a single cycle infectivity assay in presence of 10% FBS. The numbers are reported as fold shift in IC₅₀ relative to wild type HIV-1. Viruses which exhibit >50% reduction in specific infectivity (impaired replication capacity) are starred.

L-870810 is another Merck HIV strand transfer inhibitor.²⁰ S-1360 is a diketo heteroaryl derivative from Shionogi that was in clinical development. Comparing the four agents, **27** showed a similar profile to L-870810 and was better than **11**, with all Merck compounds showing a better profile than that of S-1360.

Taking into account the intrinsic potency in the cell based assay in high serum condition, the PK profile, and the mutant profile, compound **27** was selected over **11** for further development. **27** is also called Raltegravir or MK-0518, and in October 2007 was approved by the FDA as the first HIV-integrase inhibitor for the treatment of HIV AIDS infected patients.

Conclusion

The discovery of Raltegravir (**27**) came from a series of potent and structurally new HIV-integrase inhibitors designed as valuable drug-like DKA replacements for the HCV polymerase. The knowledge of the catalytic machinery of HIV-integrase and HCV polymerase led us to test the new class against HIV-integrase. We identified a compound that was active in the enzymatic assay, and by the optimization of the antiviral activity in cell culture in the presence of 50% NHS, physicochemical properties and pharmacokinetic profiles identified a number of suitable candidates. Counterscreening and activity against a series of mutants selected in vitro was the final screening funnel and led to the identification of Raltegravir or MK-0518. Raltegravir met all preclinical criteria to be considered a very effective and safe HIV agent; the prediction of human PK provided the hypothesis that it would be a BID drug, which was later confirmed in clinical studies. Raltegravir has been

approved by the FDA as the first HIV-integrase inhibitor for the treatment of HIV AIDS.

Biology

Compounds were assessed for activity against the purified HIV-1 integrase enzyme.⁶ Integrase mediated strand transfer activity was determined as described in footnote Table 1. Compounds were also tested in HIV-1 replication assays, performed in MT-4 human T-lymphoid cells as described in ref 10. Cells were infected en masse at low multiplicity (0.01). HIV-1 replication was assessed by p24 core antigen ELISA. Control cultures in the absence of inhibitor were fully infected at 4 days.

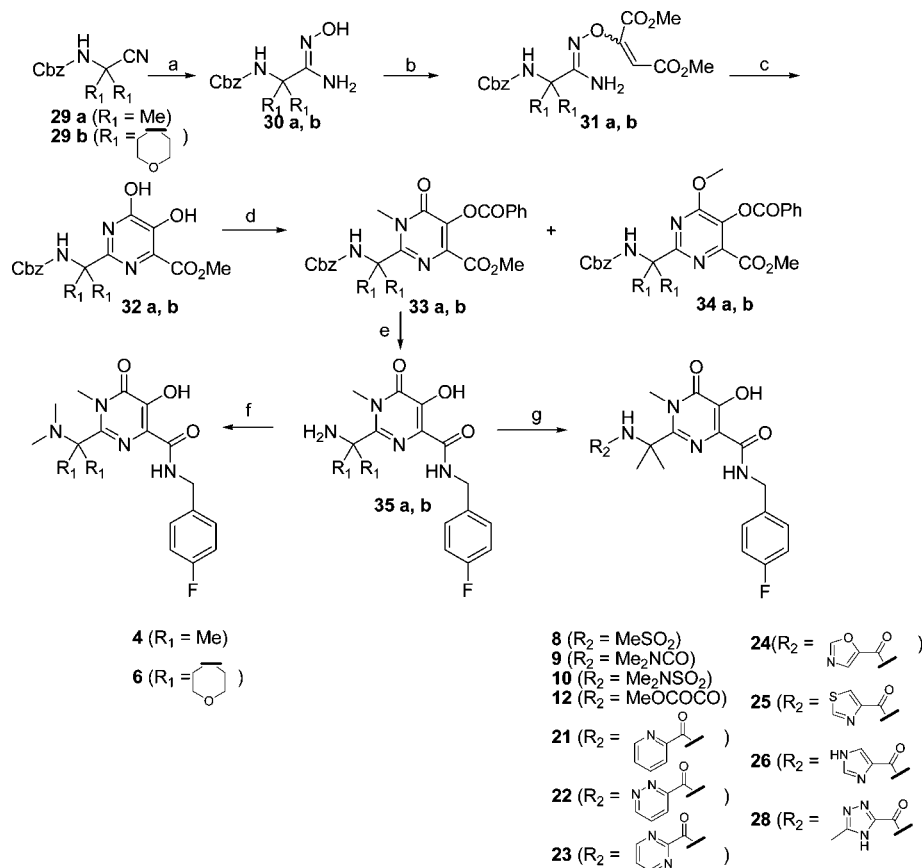
Chemistry

The general synthetic route to the core *N*-methylpyrimidone-4-carboxamide scaffold is depicted in Scheme 1. Conversion of nitriles **29** to amidoximes **30** and reaction with dimethyl acetylenedicarboxylate provided, via formation of the intermediate adducts **31**, the dihydroxypyrimidine-2-carboxylates **32**.²¹ Benzoylation of the 5-hydroxyl and subsequent methylation afforded the 2-substituted methyl 5-(benzoyloxy)-1-methyl-6-oxo-1,6-dihydropyrimidine-4-carboxylates **33** together with minor amounts of the *O*-methylated derivatives **34**, which could be easily separated via chromatography. The pyrimidones **33** were reacted with *p*-fluorobenzylamine and then hydrogenated to give the benzylic amides **35**, which served as a useful diversification point for the construction of the final compounds. Reductive amination of **35** with formaldehyde gave **4** and **6**, while sulfonamide **8**, urea **9**, sulfonyl urea **10**, and amides **12**, **21–26**, and **28** were obtained using standard protocols.

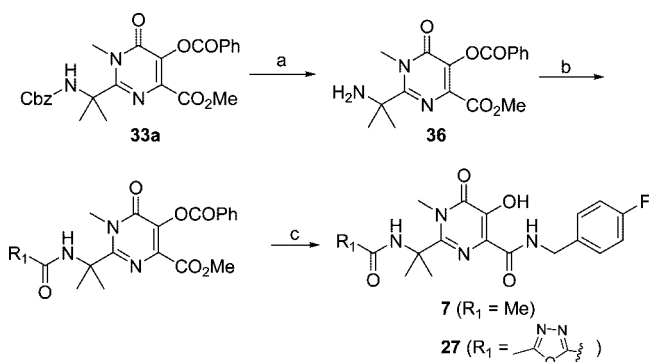
While the general synthetic route is outlined in Scheme 1, in some cases, the functionality at the amino substituent in the 2-position of the pyrimidone ring of **33a** was better introduced prior to the installation of the benzylic amide in the 4-position (Scheme 2). In particular, the synthesis of **27** by the reaction sequence in Scheme 1 gave erratic results when it was scaled up to more than one gram of material due to the acid lability of the oxadiazole ring during RP-HPLC purification. The alternative approach described in Scheme 2 allowed the removal of side products either via silica gel column chromatography or crystallization (see Experimental Section), and the synthesis could be scaled up in our laboratories to 10 g of **27** as crystalline free OH at a time.

Compound **12** was further diversified to **11**, **15**, and **16** via reaction with the appropriate amine. In some cases, the carboxylic acid **13** was isolated from the reaction mixture as a byproduct (Scheme 4). To obtain compound **14**, the same chemistry as for the preparation of **11** was applied on intermediate **37**, obtained from **35a** by a stepwise reductive amination with benzaldehyde and formaldehyde, followed by hydrogenation.

To explore the benzyl amide moiety of **11**, the reaction sequence in Scheme 5 was followed, and compounds **18–20**

Scheme 1. General Scheme for the Synthesis of *N*-Methylpyrimidone-4-carboxamides^a

^a Reagents and conditions: (a) NH₂OH.HCl, KOH, MeOH; (b) DMAD, CHCl₃, 60 °C; (c) Xylene, 150 °C; (d) i: Bz₂O, pyridine, rt; ii: Me₂SO₄, LiH, dioxane, 60 °C; (e) i: 4-F-C₆H₄CH₂NH₂, MeOH or NMP, refl.; ii: H₂, Pd/C, MeOH; (f) HCHO, NaCNBH₃, AcOH, Et₃N (or NaOAc), MeOH; (g) see *Experimental Section*.

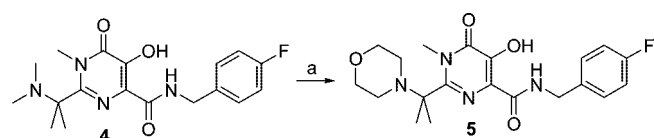
Scheme 2. Alternative Synthesis of *N*-Methylpyrimidone-4-carboxamide^a

^a Reagents and conditions: (a) H₂, Pd/C, MeOH; (b) R₁COCl, Et₃N, CH₂Cl₂; (c) ArCH₂NH₂, MeOH, refl. Compound 5 was prepared by treating 4 with an excess of morpholine in N-methylpyrrolidone at 120 °C (Scheme 3).

were prepared in parallel (as part of a larger array), with introduction of the benzylic amide as the ultimate step.

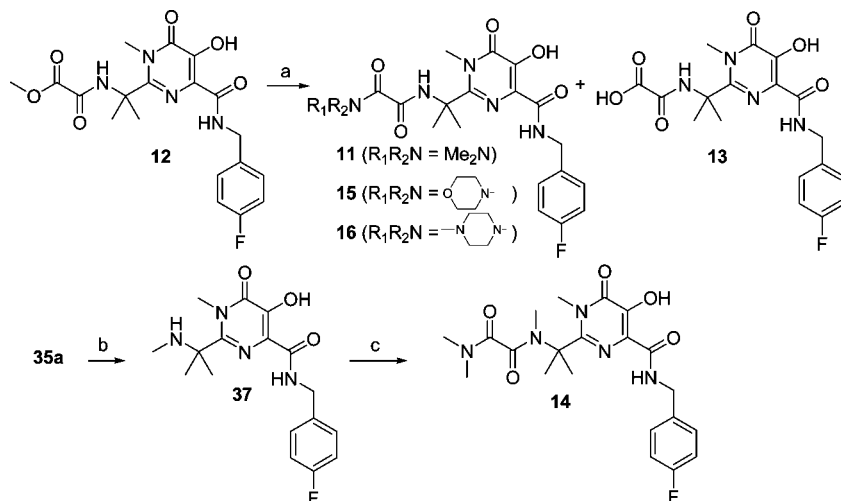
Experimental Section

Solvents and reagents were obtained from commercial suppliers and were used without further purification. Flash chromatography purifications were performed on Merck silica gel (200–400 mesh) as the stationary phase or were conducted using prepacked cartridges on a Biotage system, eluting with petroleum ether/ethyl acetate mixtures. HPLC-MS analyses were performed on a Waters Alliance

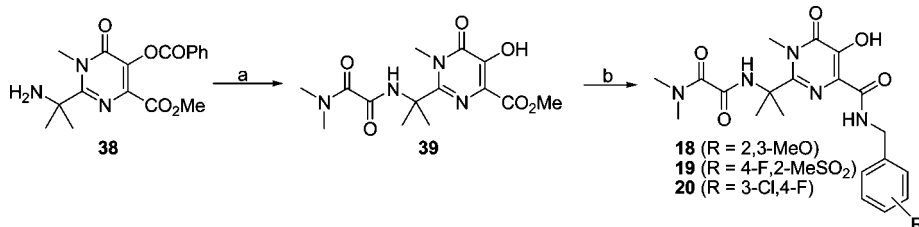
Scheme 3. Synthesis of Compound 5^a

^a Reagents and conditions: (a) Morpholine (10 equiv), NMP, 120 °C.

2795 apparatus, equipped with a diode array and a ZQ mass spectrometer, using an X-Terra C₁₈ column (5 μ m, 4.6 mm \times 50 mm). Solvent system was acetonitrile-0.1% HCOOH/water-0.1% HCOOH, gradient 10–90% over 6 min with a flow rate of 1 mL/min. Purity of final compounds was more than 99% by area. Preparative reversed-phase high-performance liquid chromatography (RP-HPLC) was performed on a Shimadzu 10AV-VP operating with a flow rate of 15 mL/min and incorporating a diode array detector SPD10AV-VP. The stationary phases used were Waters Symmetry C₁₈ 5 μ m 19 mm \times 100 mm, C₁₈ 7 μ m 19 mm \times 150 mm, and C₁₈ 7 μ m 19 mm \times 300 mm. The mobile phase comprised a linear gradient of binary mixtures of acetonitrile (containing 0.1% TFA) and H₂O (containing 0.1% TFA). Nuclear magnetic resonance spectra ¹H NMR recorded at 400 or 300 MHz, ¹³C NMR recorded at 100 or 75 MHz were obtained on Bruker AMX spectrometers and are referenced in ppm relative to TMS. Unless indicated, spectra were acquired at 300 K. Low resolution mass spectra (*m/z*) were recorded on a Perkin-Elmer API 100 (electrospray ionization) mass spectrometer. High resolution mass measurements were carried out by electrospray ionization performed on a TSQ Quantum Ultra AM operating in enhanced mass resolution mode. The accurate mass measurements were carried out on a chromatographic time scale by means of flow injection of 5 μ L of each working solution (20

Scheme 4. Synthesis of Compounds 11–16^a

^a Reagents and conditions: (a) R₁R₂N, MeOH or THF; (b) (i) PhCHO, HC(OMe)₃ then NaCNBH₃, MeOH; (ii) HCHO, NaCNBH₃; (iii) H₂, Pd/C, MeOH; (c) (i) MeOCOCOCl, Et₃N, CHCl₃; (ii) Me₂NH, THF.

Scheme 5. Synthesis of Compounds 18–20^a

^a Reagents and conditions: (a) (i) MeOCOCOCl, Et₃N, CHCl₃; (ii) Me₂NH, THF; (b) ArCH₂NH₂, NMP, 100 °C.

μg/mL concentration) in acetonitrile on a Waters C₁₈ Sunfire (20 mm × 2.1 mm, 5 μm) column using an isocratic elution (solvent A: solvent B, 50:50) of solvent A: water + 0.1% formic acid and solvent B: acetonitrile + 0.1% formic acid at a flow rate of 1000 μL/min.²²

Benzyl 1-Cyano-1-methylethylcarbamate (29a). To a suspension of 2-amino-2-methylpropanenitrile²³ (0.5 mol) in water (200 mL) an equimolar amount of Na₂CO₃ (52 g, 0.5 mol) and a slight excess (1.1 equiv) of benzylchloroformate were added with external cooling. The reaction mixture was stirred overnight at room temperature, extracted in EtOAc, and the organic phase was washed with NaHCO₃ss, dried (Na₂SO₄), filtered, and concentrated. Title product was obtained as a white solid (92 g, 0.43 mol, 85% yield). ¹H NMR (CDCl₃) δ 7.48–7.33 (bs, 5 H), 5.15 (s, 2 H), 4.98 (bs, 1 H), 1.68 (s, 6 H). ¹³C NMR (CDCl₃) δ 153.33, 13.81, 127.81, 127.63, 127.55, 120.64, 66.56, 46.19, 26.67. MS m/z 219 (M + H)⁺.

Benzyl 2-Amino-2-(hydroxyimino)-1,1-dimethylethylcarbamate (30a). Hydroxylamine hydrochloride (30 g, 0.43 mol) in methanol (100 mL) was added to an equimolar stirred solution of potassium hydroxide in methanol (100 mL). The mixture was stirred for 15 min and the precipitated potassium chloride was removed by filtration. The filtrate was added to an equimolar amount of the above nitrile **29a**, and the solution was stirred overnight at 40 °C, then cooled to room temperature and concentrated. The resulting residue was triturated with water giving, after drying under vacuum, a white solid consisting mainly of the title product **30a** (95 g, 0.38 mol, 88% yield). ¹H NMR (DMSO-d₆) δ 9.12 (bs, 1 H), 7.48 (bs, 5 H), 7.08 (bs, 1 H), 5.33 (bs, 2 H), 4.98 (s, 2 H), 1.39 (s, 6 H). MS m/z 252 (M + H)⁺.

Methyl 2-(1-[(Benzoyloxy)carbonyl]amino)-1-methylethyl)-5,6-dihydroxypyrimidine-4-carboxylate (32a). Benzyl 2-amino-2-(hydroxyimino)-1,1-dimethylethylcarbamate (**30a**, 0.38 mol) was suspended in chloroform (200 mL) and treated with 1.2 equiv of

dimethylacetylenedicarboxylate and the reaction was refluxed overnight. After cooling to room temperature, volatiles were evaporated and the residue containing crude **31a** was taken into xylene and heated at 145 °C for 48 h. The reaction mixture was stirred at room temperature overnight to allow the precipitation of the product (**32a**) as a light-brown solid. This solid was collected by filtration and washed with diethyl ether (56 g, 0.16 mol, 41% yield). ¹H NMR (DMSO-d₆) δ 12.54 (s, 1 H), 10.21 (s, 1 H), 7.44 (bs, 1 H), 7.30 (bs, 5 H), 4.95 (s, 2 H), 3.80 (s, 3 H), 1.47 (s, 6 H). MS m/z 362 (M + H)⁺.

Methyl 2-(4-[(Benzoyloxy)carbonyl]amino)tetrahydro-2H-pyran-4-yl)-5,6-dihydroxypyrimidine-4-carboxylate (32b). was prepared from benzyl (4-cyanotetrahydro-2H-pyran-4-yl)carbamate **29b** as described for the synthesis of **32a**. ¹H NMR (DMSO-d₆) δ 12.58 (s, 1H), 10.30 (s, 1H), 7.45 (bs, 1H), 7.40–7.31 (m, 5H), 4.98 (s, 2H), 3.82 (s, 3H), 3.66–3.62 (m, 4H), 2.20–2.09 (m, 2H), 1.97–1.93 (m, 2H). MS m/z 404 (M + H)⁺.

Methyl 5-(Benzoyloxy)-2-(1-[(Benzoyloxy)carbonyl]amino)-1-methylethyl)-1-methyl-6-oxo-1,6-dihydroxypyrimidine-4-carboxylate (33a). Step 1: to a stirred solution of methyl 2-(1-[(Benzoyloxy)carbonyl]amino)-1-methylethyl)-5,6-dihydroxypyrimidine-4-carboxylate **32a** (6.0 g, 16.6 mmol) in pyridine (20 mL), 1.1 equiv of benzoic anhydride was added and the resulting mixture was stirred at room temperature overnight. Pyridine was evaporated, and the residue was taken into ethyl acetate and washed with 1 N HCl and brine. The organic layer was separated, dried (Na₂SO₄), filtered, and concentrated by rotary evaporation. The residue was purified by flash column chromatography (SiO₂, petroleum ether/ethyl acetate 60/40 v/v as eluent) to give methyl 5-(benzoyloxy)-2-(1-[(Benzoyloxy)carbonyl]amino)-1-methylethyl)-6-hydroxypyrimidine-4-carboxylate (85% yield). ¹H NMR (CDCl₃) δ 12.2 (bs, 1 H), 8.15 (d, J = 7.4 Hz, 2 H), 7.65 (t, J = 7.4 Hz, 1 H), 7.50 (t, J = 7.5 Hz, 2 H), 7.32 (bs, 5 H), 5.54 (bs, 1 H), 5.05 (s, 2 H), 3.82 (s, 3 H), 1.67 (s, 6 H). MS m/z 466 (M + H)⁺. Step 2: To a stirred solution

of LiH (1.1 equiv) in dioxane (15 mL), the previous intermediate (6.5 g, 14 mmol) was added and the mixture was stirred at 38 °C for 45 min. After cooling to room temperature, dimethyl sulfate (1.3 equiv) was added and the reaction mixture was heated at 60 °C for 2 h. The mixture was then cooled to room temperature, dioxane evaporated, and the residue was purified by flash chromatography (SiO₂), eluting with 65/55 v/v petroleum ether/ethyl acetate to give **33a** (4.5 g, 67% yield). ¹H NMR (CDCl₃) δ 8.19 (d, *J* = 7.3 Hz, 2 H), 7.65 (t, *J* = 7.3 Hz, 1 H), 7.51 (t, *J* = 7.6 Hz, 2 H), 7.33 (bs, 5 H), 5.63 (bs, 1 H), 5.03 (s, 2 H), 3.80 (s, 3 H), 3.63 (bs, 3 H), 1.72 (s, 6 H). MS *m/z* 480 (M + H)⁺.

Methyl 5-(Benzoyloxy)-2-(4-[(benzyloxy)carbonyl]amino)tetrahydro-2H-pyran-4-yl)-1-methyl-6-oxo-1,6-dihydropyrimidine-4-carboxylate (33b). was prepared in 54% yield from **32b** following the same procedure described for **33a**. ¹H NMR (DMSO-*d*₆) δ 8.39 (bs, 1 H), 8.10 (d, *J* = 7.6 Hz, 2 H), 7.79 (t, *J* = 7.6 Hz, 1 H), 7.64 (t, *J* = 7.6 Hz, 2 H), 7.42–7.28 (m, 5 H), 5.02 (s, 2 H), 3.78 (s, 3 H), 3.77–3.65 (m, 4 H), 3.54 (s, 3 H), 2.34–2.27 (m, 2 H), 2.09–2.04 (m, 2 H). MS *m/z* 522 (M + H)⁺.

2-(1-Amino-1-methylethyl)-*N*-(4-fluorobenzyl)-5-hydroxy-1-methyl-6-oxo-1,6-dihydropyrimidine-4-carboxamide (35a). Step 1: to a methanolic solution of **33a** (4.5 g, 9.3 mmol), *p*-fluorobenzylamine (3 equiv) was added and the resulting mixture was refluxed overnight. After evaporation of methanol, the residue was taken into EtOAc, washed with aq 1 N HCl and brine, dried (Na₂SO₄), filtered, and evaporated to obtain benzyl 1-(4-[(4-fluorobenzyl)amino]carbonyl)-5-hydroxy-1-methyl-6-oxo-1,6-dihydropyrimidin-2-yl)-1-methylethylcarbamate (98% yield). ¹H NMR (CDCl₃) δ 11.9 (bs, 1 H), 7.79 (bt, 1 H), 7.35–7.29 (m, 7 H), 7.07 (t, *J* = 8.6 Hz, 2 H), 5.27 (bs, 1 H), 5.02 (bs, 2 H), 4.58 (d, *J* = 6.2 Hz, 2 H), 3.67 (s, 3 H), 1.70 (s, 6 H). MS *m/z* 469 (M + H)⁺. Step 2: a methanolic solution of compound from step 1 was stirred overnight under a hydrogen atmosphere in the presence of catalytic 10% Pd/C. Catalyst was then filtered off through celite, and the filtrate was concentrated. The title product was obtained after trituration with ethyl ether (100% yield). ¹H NMR (DMSO-*d*₆) δ 12.31 (bs, 1 H), 9.68 (bt, *J* = 6.6 Hz, 1 H), 8.60 (bs, 2 H), 7.43 (dd, *J* = 8.4 Hz, *J* = 5.7 Hz, 2 H), 7.20 (t, *J* = 8.8 Hz, 2 H), 4.54 (d, *J* = 6.6 Hz, 2 H), 3.56 (s, 3 H), 1.73 (s, 6 H). MS *m/z* 335 (M + H)⁺.

2-(4-Aminotetrahydro-2H-pyran-4-yl)-*N*-(4-fluorobenzyl)-5-hydroxy-1-methyl-6-oxo-1,6-dihydropyrimidine-4-carboxamide (35b). The title compound was obtained as described for the preparation of **35a**, using in step 1 methyl 5-(benzyloxy)-2-(4-[(benzyloxy)carbonyl]amino)tetrahydro-2H-pyran-4-yl)-1-methyl-6-oxo-1,6-dihydropyrimidine-4-carboxylate (**33b**). ¹H NMR (DMSO-*d*₆) δ 12.38 (bs, 1 H), 9.82 (bs, 1 H), 8.98 (s, 2 H), 7.50–7.45 (m, 2 H), 7.25–7.19 (m, 2 H), 4.57 (d, *J* = 6.2 Hz, 2 H), 3.95–3.88 (m, 4 H), 3.66 (s, 3 H), 2.72–2.58 (m, 2 H), 1.85–1.79 (m, 2 H). MS *m/z* 377 (M + H)⁺.

2-[5-(Benzoyloxy)-4-(methoxycarbonyl)-1-methyl-6-oxo-1,6-dihydropyrimidin-2-yl]propan-2-amine Hydrochloride (36). A solution of methyl 5-(benzyloxy)-2-(1-[(benzyloxy)carbonyl]amino)-1-methylethyl)-1-methyl-6-oxo-1,6-dihydropyrimidine-4-carboxylate (**33a**) (3.86 g, 8.06 mmol) in MeOH (160 mL) and 1 equiv of 6 N HCl (1.34 mL) was stirred in the presence of 10% Pd/C (400 mg) under an H₂ atmosphere at atmospheric pressure for 90 min. The mixture was then filtered and the Pd residues washed with MeOH (150 mL). The combined organics were concentrated under reduced pressure to yield the title compound as hydrochloride salt (3.08 g, quantitative yield). ¹H NMR (DMSO-*d*₆) δ 8.72 (br, s, 3 H), 8.09 (d, *J* = 7.5 Hz, 2 H), 7.80 (t, *J* = 7.5 Hz, 1 H), 7.64 (t, *J* = 7.5 Hz, 2 H), 3.79 (s, 3 H), 3.63 (s, 3 H), 1.84 (s, 6 H). MS *m/z* 346 (M + H)⁺.

2-[1-(Dimethylamino)-1-methylethyl]-*N*-(4-fluorobenzyl)-5-hydroxy-1-methyl-6-oxo-1,6-dihydropyrimidine-4-carboxamide (4). To a stirred solution of **35a** in methanol, 1.5 equiv of acetic acid were added followed by NaBH₃CN (2 equiv) and formaldehyde (37% aqueous solution, 2.5 equiv). The mixture was stirred at room temperature for 2 h, concentrated by rotary evaporation, and purified by preparative RP-HPLC (C₁₈, water/acetonitrile with 0.1% trifluoroacetic acid as eluent). Collection and lyophilization of appropriate fractions afforded compound **4** as its trifluoroacetate salt (23% yield). ¹H NMR (DMSO-*d*₆) δ 12.58 (bs, 1 H), 9.71 (bt, *J* = 6.6 Hz, 1 H), 9.37 (bs, 1 H), 7.37 (dd, *J* = 8.4, 5.7 Hz, 2 H), 7.19 (t, *J* = 8.8 Hz, 2 H), 4.48 (d, *J* = 6.6 Hz, 2 H), 3.56 (s, 3 H), 2.79 (s, 6 H), 1.72 (s, 6 H). MS *m/z* 363 (M + H)⁺. HRMS calcd for C₁₈H₂₄O₄N₄F (M + H)⁺: 363.18270. Found: 363.18274.

N-(4-Fluorobenzyl)-5-hydroxy-1-methyl-2-(1-methyl-1-morpholin-4-ylethyl)-6-oxo-1,6-dihydropyrimidine-4-carboxamide (5). A solution of **4** (25 mg, 0.052 mmol) in *N*-methylpyrrolidone (1 mL) was treated with 20 equiv of morpholine and the mixture was stirred at 120 °C for 2 days, then cooled to room temperature and purified by preparative RP-HPLC (C₁₈, water/acetonitrile with 0.1% trifluoroacetic acid as eluent) to give **5** as its trifluoroacetate salt (15 mg, 56% yield). ¹H NMR (DMSO-*d*₆) δ 12.20 (bs, 1 H), 8.96 (bt, *J* = 6.9 Hz, 1 H), 7.49 (dd, *J* = 8.5, 5.6 Hz, 2 H), 7.18 (t, *J* = 8.8 Hz, 2 H), 4.50 (d, *J* = 6.9 Hz, 2 H), 3.98 (s, 3 H), 3.57 (bs, 4 H), 2.44 (bs, 4 H), 1.44 (s, 6 H). MS *m/z* 405 (M + H)⁺. HRMS calcd for C₂₀H₂₆O₄N₄F (M + H)⁺: 405.19326. Found: 405.19302.

2-[4-(Dimethylamino)tetrahydro-2H-pyran-4-yl]-*N*-(4-fluorobenzyl)-5-hydroxy-1-methyl-6-oxo-1,6-dihydropyrimidine-4-carboxamide (6). A solution of **35b** (0.05 g, 0.1 mmol) in MeOH (1 mL) was treated with triethylamine (0.017 mL, 0.12 mmol), sodium acetate (0.013 g, 0.16 mmol), formaldehyde 37% w/w aq soln (0.022 mL, 0.3 mmol), and sodium cyanoborohydride (0.009 g, 0.14 mmol). The mixture was stirred at room temperature for 3 h. Volatiles were removed under vacuum and the crude was purified by preparative RP-HPLC, giving the title compound **6** as trifluoroacetate salt. ¹H NMR (CD₃CN + TFA) δ 8.33 (bt, 1 H), 7.57–7.52 (m, 2 H), 7.29–7.23 (m, 2 H), 4.75 (d, *J* = 6.6 Hz, 2 H), 4.18–4.09 (m, 2 H), 3.80 (s, 3 H), 3.63–3.58 (m, 2 H), 3.08–3.03 (m, 8 H), 2.40–2.30 (m, 2 H). MS *m/z* 405 (M + H)⁺. HRMS calcd for C₂₀H₂₆O₄N₄F (M + H)⁺: 405.19326. Found: 405.19290.

2-[1-(Acetylamino)-1-methylethyl]-*N*-(4-fluorobenzyl)-5-hydroxy-1-methyl-6-oxo-1,6-dihydropyrimidine-4-carboxamide (7). To a stirred solution of **36** (0.14 mmol) and triethylamine (6 equiv) in dichloromethane (1 mL), 3 equiv of acetyl chloride were added. The mixture was stirred at room temperature for 3 h then diluted with chloroform and washed with 1 N HCl, brine, and NaHCO₃. The dried organic phase was concentrated, and the residue was taken up in methanol (1 mL) and treated with 2.5 equiv of *p*-fluorobenzylamine. The mixture was refluxed for 4 h then purified by preparative RP-HPLC to give the title compound in 14% yield. ¹H NMR (DMSO-*d*₆) δ 12.11 (bs, 1 H), 8.99 (bt, *J* = 5.7 Hz, 1 H), 8.43 (s, 1 H), 7.48 (dd, *J* = 8.5, 5.7 Hz, 2 H), 7.17 (t, *J* = 8.8 Hz, 2 H), 4.49 (d, *J* = 5.7 Hz, 2 H), 3.48 (s, 3 H), 1.84 (s, 3 H), 1.59 (s, 6 H). MS *m/z* 377 (M + H)⁺. HRMS calcd for C₁₈H₂₂O₄N₄F (M + H)⁺: 377.16196. Found: 377.16203.

N-(4-Fluorobenzyl)-5-hydroxy-1-methyl-2-(1-methyl-1-[methylsulfonyl]aminoethyl)-6-oxo-1,6-dihydropyrimidine-4-carboxamide (8). Methyl sulfonyl chloride (0.028 mL, 0.36 mmol, 1.2 equiv) was added dropwise to a solution of **35a** (0.1 g, 0.30 mmol, 1.0 equiv) and Et₃N (0.050 mL, 0.36 mmol, 1.2 equiv) in dichloromethane (10 mL) at 0 °C, and stirring was continued at room temperature. After 1 h, volatiles were evaporated in vacuum, the residue was dissolved in dimethylamine (5 mL, 2.0 M solution in THF), and stirring was continued overnight. The solvent was reduced in vacuo, and the residue was dissolved in EtOAc, washed with 1 N HCl and brine, and dried over Na₂SO₄. Evaporation of the solvent gave a residue, which was purified by preparative RP-HPLC, yielding **8** as a solid (0.043 g, 35% yield). ¹H NMR (DMSO-*d*₆ + TFA) δ 12.14 (bs, 1 H), 8.98 (t, *J* = 6.2 Hz, 1 H), 7.81 (s, 1 H), 7.38 (dd, *J* = 8.4, 5.8 Hz, 2 H), 7.16 (t, *J* = 8.8 Hz, 2 H), 4.49 (d, *J* = 6.4 Hz, 2 H), 3.68 (s, 3 H), 3.00 (s, 3 H), 1.70 (s, 6 H). MS *m/z* 413 (M + H)⁺. HRMS calcd for C₁₇H₂₂O₅N₄FS (M + H)⁺: 413.12895. Found: 413.12906.

2-(1-[(Dimethylamino)carbonyl]amino)-1-methylethyl)-*N*-(4-fluorobenzyl)-5-hydroxy-1-methyl-6-oxo-1,6-dihydropyrimidine-4-carboxamide (9). A solution of **35a** (0.038 g) in dichloromethane (2 mL) was added to a solution of di-*tert*-butyl dicarbonate (1.4

equiv) and DMAP (1.0 equiv) in dichloromethane (1 mL), and the reaction mixture was stirred for 30 min at room temperature. Then a 2 M solution of dimethylamine in THF (2.0 equiv) was added, and the mixture was stirred at 40 °C for 2 h. After evaporation of volatiles, the residue was purified by preparative RP-HPLC to give compound **9** in 23% yield. ¹H NMR (DMSO-*d*₆) δ 12.07 (bs, 1 H), 8.94 (t, *J* = 7.0 Hz, 1 H), 7.49 (dd, *J* = 8.5, 5.6 Hz, 2 H), 7.17 (t, *J* = 8.8 Hz, 2 H), 6.52 (s, 1 H), 4.51 (d, *J* = 7.0 Hz, 2 H), 3.53 (s, 3 H), 2.79 (s, 6 H), 1.62 (s, 6 H); MS *m/z* 406 (M + H)⁺. HRMS calcd for C₁₉H₂₅O₄N₅F (M + H)⁺: 406.18851. Found: 406.18753.

2-(1-[(Dimethylamino)sulfonyl]amino)-1-methylethyl)-N-(4-fluorobenzyl)-5-hydroxy-1-methyl-6-oxo-1,6-dihydropyrimidine-4-carboxamide (10). To a solution of **35a** (100 mg, 0.30 mmol, 1.0 equiv) and Et₃N (0.05 mL, 0.35 mmol, 1.2 equiv) in dichloromethane (10 mL), dimethylsulfonyl chloride (0.038 mL, 0.35 mmol, 1.2 equiv) was added. After stirring for 18 h at room temperature, volatiles were evaporated in vacuo, the residue was dissolved in dimethylamine (5 mL, 2.0 M in THF), and stirring was continued overnight. The solvent was reduced in vacuo and the residue was dissolved in EtOAc, washed with 1 N HCl and brine, and dried over Na₂SO₄. After evaporation of volatiles, crude was purified by RP-HPLC to give compound **10**. ¹H NMR (DMSO-*d*₆) δ 12.20 (bs, 1 H), 8.97 (t, *J* = 6.2 Hz, 1 H), 7.63 (s, 1 H), 7.37 (dd, *J* = 8.6, 5.7 Hz, 2 H), 7.16 (t, *J* = 9.1 Hz, 2 H), 4.49 (d, *J* = 6.4 Hz, 2 H), 3.72 (s, 3 H), 2.66 (s, 6 H), 1.67 (s, 6 H). MS *m/z* 442 (M + H)⁺.

Methyl {[1-(4-[(4-Fluorobenzyl)amino]carbonyl)-5-hydroxy-1-methyl-6-oxo-1,6-dihydropyrimidin-2-yl]-1-methylethyl}-amino}(oxo)acetate (12). To a stirred mixture of **35a** (3.44 g, 9.3 mmol) and triethylamine (3 equiv) in chloroform (20 mL), methyl chloroxoacetate (1.5 equiv) was added with external cooling. After the addition, the ice bath was removed and the mixture was stirred at room temperature for 3 h. Reaction mixture was then partitioned between chloroform and 1 N HCl. Organic layer was separated, washed with brine, dried (Na₂SO₄), filtered, and concentrated to obtain title product **12** (80% yield). An aliquot of the crude product was further purified by preparative RP-HPLC. ¹H NMR (DMSO-*d*₆) δ 12.2 (bs, 1 H), 9.47 (s, 1 H), 9.04 (t, *J* = 6.3 Hz, 1 H), 7.38 (dd, *J* = 8.4 Hz, *J* = 5.7 Hz, 2 H), 7.16 (t, *J* = 8.8 Hz, 2 H), 4.50 (d, *J* = 6.3 Hz, 2 H), 3.78 (s, 3 H), 3.45 (s, 3 H), 1.67 (s, 6 H). MS *m/z* 421 (M + H)⁺. HRMS calcd for C₁₉H₂₂O₆N₄F (M + H)⁺: 421.15179. Found: 421.15140.

N-[1-(4-[(4-Fluorobenzyl)amino]carbonyl)-5-hydroxy-1-methyl-6-oxo-1,6-dihydropyrimidin-2-yl]-1-methylethyl]-*N,N*-dimethylethanediamide (11). Compound **12** (3.14 g, 7.5 mmol) was refluxed in an excess of 2 M solution of dimethylamine in THF for 2 h. The reaction mixture was cooled to room temperature, evaporated, and the residue was purified by RP-HPLC (C₁₈, water/acetonitrile containing 0.1% of trifluoroacetic acid as eluent) to give **11** in 75% yield. ¹H NMR (DMSO-*d*₆) δ 12.19 (s, 1 H), 9.32 (s, 1 H), 9.06 (t, *J* = 6.4 Hz, 1 H), 7.40 (dd, *J* = 8.5, 5.7 Hz, 2 H), 7.18 (t, *J* = 8.8 Hz, 2 H), 4.51 (d, *J* = 6.4 Hz, 2 H), 3.55 (s, 3 H), 2.93 (s, 3 H), 2.87 (s, 3 H), 1.68 (s, 6 H). ¹³C NMR (DMSO-*d*₆) δ 168.23, 163.76, 163.09, 161.20 (d, *J* = 96.4 Hz), 158.46, 151.90, 145.49, 134.77, 129.40 (d, *J* = 3.2 Hz), 124.29, 115.05 (d, *J* = 8.5 Hz), 56.50, 41.51, 35.46, 33.42, 32.68, 26.85. ¹⁹F-NMR (DMSO-*d*₆) δ -116.71. MS *m/z* 434 (M + H)⁺; mp (Na⁺ salt): 199–201 °C. HRMS calcd for C₂₀H₂₅O₅N₅F (M + H)⁺: 434.18342. Found: 434.18357.

N-[1-(4-[(4-Fluorobenzyl)amino]carbonyl)-5-hydroxy-1-methyl-6-oxo-1,6-dihydropyrimidin-2-yl]-1-methylethyl]-*N,N'*-trimethylethanediamide (14). Step 1: 2-{1-[Benzyl(methyl)amino]-1-methylethyl}-N-(4-fluorobenzyl)-5-hydroxy-1-methyl-6-oxo-1,6-dihydropyrimidine-4-carboxamide. A solution of **35a** (0.33 g, 0.89 mmol) in trimethylorthoformate (5 mL) was treated with 4 equiv of benzaldehyde, and the mixture stirred for two days at room temperature. Volatiles were evaporated, and the residue was taken up in methanol and 1 equiv of NaCNBH₃ was added. After 1.5 h stirring, 2 equiv of formaldehyde and an additional 2 equiv of NaCNBH₃ were added and the resulting mixture was left overnight at room temperature. The crude mixture was then acidified with

some drops of 1 N HCl and charged on cation-exchange resin cartridges (Varian Mega Bond Elute SCX). The cartridges were washed with MeOH, and the crude product was eluted with 1 M ammonia in methanol. The pooled eluents were concentrated to dryness under reduced pressure to give a solid-pink residue containing the title product (0.280 g, 72% yield). MS *m/z* 439 (M + H)⁺. Step 2: *N*-(4-fluorobenzyl)-5-hydroxy-1-methyl-2-[1-methyl-1-(methylamino)ethyl]-6-oxo-1,6-dihydropyrimidine-4-carboxamide. Compound from previous step (0.28 g, 0.64 mmol) was taken up in methanol (10 mL) and hydrogenated under hydrogen atmosphere in the presence of 10% Pd/C. After overnight stirring, the catalyst was filtered off and the filtrate concentrated under reduced pressure after addition of a few drops of 1 N HCl. Product was obtained by trituration with diethyl ether as a white solid (HCl salt, 98% yield). ¹H NMR (DMSO-*d*₆, 330 K) δ 12.39 (bs, 1 H), 9.90 (bs, 1 H), 9.42 (bs, 2 H), 7.43 (m, 2 H), 7.14 (t, *J* = 8.7 Hz, 2 H), 4.52 (d, *J* = 6.7 Hz, 2 H), 3.54 (s, 3 H), 2.57 (s, 3 H), 1.77 (s, 6 H). MS *m/z* 349 (M + H)⁺. Step 3: following the same procedure described for **12**, treatment of *N*-(4-fluorobenzyl)-5-hydroxy-1-methyl-2-[1-methyl-1-(methylamino)ethyl]-6-oxo-1,6-dihydropyrimidine-4-carboxamide from above with methyl chloroxoacetate gave a residue that was reacted with dimethylamine as described for **11**. Purification by preparative RP-HPLC afforded **14** in 56% yield. ¹H NMR (DMSO-*d*₆, 330 K) δ 12.09 (bs, 1 H), 9.03 (t, *J* = 5.9 Hz, 1 H), 7.39 (dd, *J* = 8.5, 5.7 Hz, 2 H), 7.14 (t, *J* = 8.8 Hz, 2 H), 4.52 (d, *J* = 5.9 Hz, 2 H), 3.43 (s, 3 H), 3.01 (s, 3 H), 2.87 (s, 3 H), 2.86 (s, 3 H), 1.68 (s, 6 H). MS *m/z* 448 (M + H)⁺. HRMS calcd for C₂₁H₂₇O₅N₅F (M + H)⁺: 448.19907. Found: 448.19934.

N-(4-Fluorobenzyl)-5-hydroxy-1-methyl-2-(1-methyl-1-[(morpholin-4-yl)(oxo)acetyl]amino)ethyl]-6-oxo-1,6-dihydropyrimidine-4-carboxamide (15). Following the same procedure described for **11**, treatment of **12** with morpholine and purification by preparative RP-HPLC gave **15** in 55% yield. ¹H NMR (DMSO-*d*₆, 330 K) δ 12.18 (bs, 1 H), 9.24 (s, 1 H), 8.89 (bt, 1 H), 7.39 (dd, *J* = 8.4, 5.4 Hz, 2 H), 7.14 (t, *J* = 8.7 Hz, 2 H), 4.51 (d, *J* = 5.6 Hz, 2 H), 3.60 (m, 4 H), 3.56 (s, 3 H), 3.49 (m, 2 H), 3.40 (m, 2 H), 1.69 (s, 6 H). MS *m/z* 476 (M + H)⁺. HRMS calcd for C₂₂H₂₇O₆N₅F (M + H)⁺: 476.19399. Found: 476.19390.

{[1-(4-[(4-Fluorobenzyl)amino]carbonyl)-5-hydroxy-1-methyl-6-oxo-1,6-dihydropyrimidin-2-yl]-1-methylethyl}amino}(oxo)acetic acid (13). The compound was isolated as byproduct of the above reaction. ¹H NMR (DMSO-*d*₆, 330 K) δ 12.20 (bs, 1 H), 9.38 (s, 1 H), 9.05 (t, *J* = 6.5 Hz, 1 H), 7.48 (dd, *J* = 8.6, 5.7 Hz, 2 H), 7.16 (t, *J* = 8.9 Hz, 2 H), 4.52 (d, *J* = 6.5 Hz, 2 H), 3.44 (s, 3 H), 1.68 (s, 6 H). MS *m/z* 407 (M + H)⁺. HRMS calcd for C₁₈H₂₀O₆N₄F (M + H)⁺: 407.13614. Found: 407.13564.

N-(4-Fluorobenzyl)-5-hydroxy-1-methyl-2-(1-methyl-1-[(4-methylpiperazin-1-yl)(oxo)acetyl]amino)ethyl]-6-oxo-1,6-dihydropyrimidine-4-carboxamide (16). Following the same procedure described for **11**, treatment of **12** with *N*-methylpiperazine and purification by preparative RP-HPLC gave **16** (as trifluoroacetic salt) in 67% yield. ¹H NMR (DMSO-*d*₆) δ 12.23 (bs, 1 H), 9.86 (bs, 1 H), 9.48 (s, 1 H), 9.04 (t, *J* = 6.9 Hz, 1 H), 7.42 (dd, *J* = 8.5, 5.7 Hz, 2 H), 7.19 (t, *J* = 8.9 Hz, 2 H), 4.56 (d, *J* = 7.0 Hz, 2 H), 4.40 (bs, 1 H), 4.00 (bs, 1 H), 3.58 (s, 3 H), 3.53 (bs, partially obscured by water, 2 H), 3.08 (bs, 4 H), 2.87 (bs, 3 H), 1.69 (s, 6 H). MS *m/z* 489 (M + H)⁺. HRMS calcd for C₂₃H₃₀O₅N₆F (M + H)⁺: 489.22562. Found: 489.22460.

N'-[1-(4-[(2,3-Dimethoxybenzyl)amino]carbonyl)-5-hydroxy-1-methyl-6-oxo-1,6-dihydropyrimidin-2-yl]-1-methylethyl]-*N,N*-dimethylethanediamide (18). As for the synthesis of **12**, replacing **35a** with **36** gave a residue that was reacted with dimethylamine as described for **11** to afford crude methyl 2-(1-[(dimethylamino)(oxo)acetyl]amino)-1-methylethyl)-5-hydroxy-1-methyl-6-oxo-1,6-dihydropyrimidine-4-carboxylate **39**. MS *m/z* 341 (M + H)⁺. A portion of this material was taken in *N*-methylpyrrolidone and treated with about 1.2 equiv of 2,3-dimethoxybenzylamine at 100 °C for 1 h. Purification by preparative RP-HPLC afforded the title compound. ¹H NMR (DMSO-*d*₆) δ 12.10 (bs, 1 H), 9.31 (s, 1 H), 8.85 (t, *J* = 7.3 Hz, 1 H), 7.05–6.96 (m, 2 H), 6.82 (dd, *J* = 8.0,

5.5 Hz, 1 H), 4.54 (d, J = 7.3 Hz, 2 H), 3.80 (s, 3 H), 3.78 (s, 3 H), 2.92 (s, 3 H), 2.86 (s, 3 H), 1.68 (s, 6 H). MS m/z 476 (M + H)⁺. HRMS calcd for C₂₂H₃₀O₇N₅ (M + H)⁺: 476.21398. Found: 476.21387.

N'-{1-[4-({[4-Fluoro-2-(methylsulfonyl)benzyl]amino}carbonyl)-5-hydroxy-1-methyl-6-oxo-1,6-dihydropyrimidin-2-yl]-1-methylethyl}-N,N-dimethylethanediamide (19). As for the synthesis of **18**, treatment of crude **39** with 4-fluoro-2-(methylsulfonyl)benzylamine followed by preparative RP-HPLC afforded the title compound. ¹H NMR (DMSO-*d*₆) δ 11.78 (bs, 1 H), 9.36 (s, 1 H), 9.00 (t, J = 6.9 Hz, 1 H), 7.72 (m, 1 H), 7.67–7.59 (m, 2 H), 4.86 (d, J = 6.9 Hz, 2 H), 3.54 (s, 3 H), 2.93 (s, 3 H), 2.87 (s, 3 H), 1.68 (s, 6 H), a methyl signal obscured by water. MS m/z 512 (M + H)⁺. HRMS calcd for C₂₁H₂₇O₇N₅FS (M + H)⁺: 512.16152. Found: 512.16148.

N'-[1-4-({[3-Chloro-4-fluorobenzyl]amino}carbonyl)-5-hydroxy-1-methyl-6-oxo-1,6-dihydropyrimidin-2-yl]-1-methylethyl]-N,N-dimethylethanediamide (20). As for the synthesis of **18**, treatment of crude **39** with 3-chloro-4-fluorobenzylamine followed by preparative RP-HPLC afforded the title compound. ¹H NMR (DMSO-*d*₆) δ 12.03 (bs, 1 H), 9.31 (s, 1 H), 9.08 (t, J = 6.4 Hz, 1 H), 7.55 (d, J = 5.6 Hz, 1 H), 7.40–7.37 (m, 2 H), 4.49 (d, J = 6.4 Hz, 2 H), 3.54 (s, 3 H), 2.91 (s, 3 H), 2.85 (s, 3 H), 1.67 (s, 6 H). MS m/z 468 (M + H)⁺. HRMS calcd for C₂₀H₂₄O₅N₅ClF (M + H)⁺: 468.14445. Found: 468.14464.

N-(4-Fluorobenzyl)-5-hydroxy-1-methyl-2-[1-methyl-1-[(pyridin-2-ylcarbonyl)amino]ethyl]-6-oxo-1,6-dihydropyrimidine-4-carboxamide (21). A solution of **35a** (0.040 g, 0.11 mmol) in chloroform (1 mL) was treated with pyridine-2-carboxylic acid (0.027 g, 0.22 mmol), EDCI (0.041 g, 0.022 mmol), HOBT (0.033 g, 0.22 mmol), and *N,N*-diisopropylethylamine (0.22 mmol). The mixture was stirred for 24 h, then concentrated and purified by preparative RP-HPLC to give **22** in 62% yield. ¹H NMR (DMSO-*d*₆) δ 12.16 (bs, 1 H), 9.16 (s, 1 H), 9.07 (t, J = 6.5 Hz, 1 H), 8.68 (d, J = 3.6 Hz, 1 H), 8.02 (dd, J = 6.8, 7.6 Hz, 1 H), 7.92 (d, J = 6.8 Hz, 1 H), 7.63 (dd, J = 7.6, 3.6 Hz, 1 H), 7.48 (dd, J = 8.6, 5.4 Hz, 2 H), 7.27 (t, J = 8.8 Hz, 2 H), 4.53 (d, J = 6.5 Hz, 2 H), 3.46 (s, 3 H), 1.75 (s, 6 H). MS m/z 440 (M + H)⁺. HRMS calcd for C₂₂H₂₃O₄N₅F (M + H)⁺: 440.17286. Found: 440.17206.

N-[1-4-({[4-Fluorobenzyl]amino}carbonyl)-5-hydroxy-1-methyl-6-oxo-1,6-dihydropyrimidin-2-yl]-1-methylethyl]pyridazine-3-carboxamide (22). Following the procedure described for **21**, treatment of **35a** with pyridazine-3-carboxylic acid and purification by preparative RP-HPLC afforded the title compound in 25% yield. ¹H NMR (DMSO-*d*₆) δ 12.18 (bs, 1 H), 9.68 (s, 1 H), 9.43 (dd, J = 4.9, 1.8 Hz, 1 H), 9.08 (t, J = 6.7 Hz, 1 H), 8.11 (dd, J = 8.8, 1.8 Hz, 1 H), 7.91 (dd, J = 8.8, 4.9 Hz, 1 H), 7.40 (dd, J = 8.4, 5.6 Hz, 2 H), 7.27 (t, J = 8.9 Hz, 2 H), 4.54 (d, J = 6.7 Hz, 2 H), 3.49 (s, 3 H), 1.79 (s, 6 H). MS m/z 441 (M + H)⁺. HRMS calcd for C₂₁H₂₂O₄N₆F (M + H)⁺: 441.16811. Found: 441.16696.

N-[1-4-({[4-Fluorobenzyl]amino}carbonyl)-5-hydroxy-1-methyl-6-oxo-1,6-dihydropyrimidin-2-yl]-1-methylethyl]pyrimidine-2-carboxamide (23). Following the procedure described for **21**, treatment of **35a** with pyrimidine-2-carboxylic acid and purification by preparative RP-HPLC afforded the title compound in 40% yield. ¹H NMR (DMSO-*d*₆) δ 12.15 (bs, 1 H), 9.31 (s, 1 H), 9.08 (t, J = 6.2 Hz, 1 H), 8.96 (d, J = 4.9 Hz, 2 H), 7.69 (t, J = 4.9 Hz, 1 H), 7.40 (dd, J = 8.4, 5.7 Hz, 2 H), 7.17 (t, J = 8.8 Hz, 2 H), 4.52 (d, J = 6.2 Hz, 2 H), 3.50 (s, 3 H), 1.76 (s, 6 H). MS m/z 441 (M + H)⁺. HRMS calcd for C₂₁H₂₂O₄N₆F (M + H)⁺: 441.16811. Found: 441.16678.

N-(4-Fluorobenzyl)-5-hydroxy-1-methyl-2-[1-methyl-1-[(1,3-oxazol-5-ylcarbonyl)amino]ethyl]-6-oxo-1,6-dihydropyrimidine-4-carboxamide (24). Following the general procedure described for **21**, treatment of **35a** with 1,3-oxazole-5-carboxylic acid and purification by preparative RP-HPLC afforded the title compound in 33% yield. ¹H NMR (DMSO-*d*₆) δ 12.27 (bs, 1 H), 9.12 (m, 2 H), 8.63 (s, 1 H), 7.91 (s, 1 H), 7.45 (dd, J = 8.6, 5.4 Hz, 2 H), 7.23 (t, J = 8.8 Hz, 2 H), 4.57 (d, J = 6.7 Hz, 2 H), 3.51 (s, 3 H), 1.80 (s, 6 H). MS m/z 430 (M + H)⁺. HRMS calcd for C₂₀H₂₁O₅N₅F (M + H)⁺: 430.15212. Found: 430.15204.

N-(4-Fluorobenzyl)-5-hydroxy-1-methyl-2-[1-methyl-1-[(1,3-thiazol-4-ylcarbonyl)amino]ethyl]-6-oxo-1,6-dihydropyrimidine-4-carboxamide (25). Following the procedure described for **21**, treatment of **35a** with 1,3-thiazole-4-carboxylic acid and purification by preparative RP-HPLC afforded the title compound in 15% yield. ¹H NMR (DMSO-*d*₆) δ 12.15 (bs, 1 H), 9.21 (s, 1 H), 9.03 (bt, 1 H), 8.89 (s, 1 H), 8.28 (s, 1 H), 7.43–7.32 (m, 2 H), 7.17 (t, J = 8.8 Hz, 2 H), 4.51 (d, J = 6.0 Hz, 2 H), 3.48 (s, 3 H), 1.78 (s, 6 H). MS m/z 446 (M + H)⁺. HRMS calcd for C₂₀H₂₁O₄N₅FS (M + H)⁺: 446.12928. Found: 446.13049.

N-(4-Fluorobenzyl)-5-hydroxy-2-[1-[(1*H*-imidazol-5-ylcarbonyl)amino]-1-methylethyl]-1-methyl-6-oxo-1,6-dihydropyrimidine-4-carboxamide (26). Following the procedure described for **21**, treatment of **35a** with 1*H*-imidazole-5-carboxylic acid and purification by preparative RP-HPLC afforded the title compound in 15% yield. ¹H NMR (DMSO-*d*₆) δ 12.18 (bs, 1 H), 9.07 (bt, 1 H), 8.77 (bs, 1 H), 8.45 (bs, 1 H), 8.42 (bs, 1 H), 7.41 (dd, J = 8.5, 5.6 Hz, 2 H), 7.18 (t, J = 8.9 Hz, 2 H), 4.52 (d, J = 6.4 Hz, 2 H), 3.48 (s, 3 H), 1.73 (s, 6 H). MS m/z 429 (M + H)⁺. HRMS calcd for C₂₀H₂₂O₄N₆F (M + H)⁺: 429.16811. Found: 429.16754.

N-(4-Fluorobenzyl)-5-hydroxy-1-methyl-2-(1-methyl-1-[(5-methyl-1,3,4-oxadiazol-2-yl)carbonyl]amino]ethyl)-6-oxo-1,6-dihydropyrimidine-4-carboxamide (27). Step 1: to a stirred suspension of potassium 5-methyl-1,3,4-oxadiazole-2-carboxylate (2.67 g, 16.1 mmol) in dichloromethane (300 mL) at room temperature, a solution of oxalyl chloride (32.2 mmol) in dichloromethane (2.0 M, 16.1 mL) was added dropwise over 10 min. DMF (15 drops, ca. 0.1 mL) was added, and vigorous gas evolution was observed. The resulting reaction mixture was stirred for a further 30 min, after which time a second portion of DMF (ca. 0.1 mL) was added and stirring was continued for a further hour, by which point almost the entire solid had dissolved. The reaction mixture was then concentrated under reduced pressure. Meanwhile, 2-[5-(benzoyloxy)-4-(methoxycarbonyl)-1-methyl-6-oxo-1,6-dihydropyrimidin-2-yl]propan-2-amine hydrochloride (**36**, 3.08 g, 8.05 mmol) was taken up in dichloromethane (300 mL) and Et₃N (4.49 mL, 32.2 mmol) and cloudy solution of the freshly prepared 5-methyl-1,3,4-oxadiazole-2-carbonyl chloride in dichloromethane (150 mL) was added dropwise over 15 min. The resulting solution was stirred for a further hour, and then the mixture was washed with saturated aq NaHCO₃ solution (150 mL), H₂O (150 mL), and brine (150 mL). The mixture was dried (Na₂SO₄) and concentrated under reduced pressure. The material was purified by column chromatography on silica using 100% EtOAc as eluent to yield methyl 5-(benzoyloxy)-1-methyl-2-(1-methyl-1-[(5-methyl-1,3,4-oxadiazol-2-yl)carbonyl]amino]ethyl)-6-oxo-1,6-dihydropyrimidine-4-carboxylate. (2.85 g, 78%). ¹H NMR (DMSO-*d*₆) δ 10.02 (bs, 1 H), 8.09 (d, J = 7.5 Hz, 2 H), 7.76 (t, J = 7.5 Hz, 1 H), 7.63 (t, J = 7.5 Hz, 2 H), 3.77 (s, 3 H), 3.56 (s, 3 H), 2.58 (s, 3 H), 1.75 (s, 6 H). MS m/z 456 (M + H)⁺. Step 2: a mixture of compound from previous step (2.85 g, 6.25 mmol) and 4-fluorobenzyl amine (1.72 mL, 15.0 mmol) in MeOH (50 mL) was heated at reflux for 14 h, then cooled to room temperature and concentrated under reduced pressure. The resulting mixture was taken up in 0.5 N NaOH solution (240 mL) and was washed with Et₂O (3 \times 200 mL). The aqueous layer was cautiously neutralized with 6 N HCl solution (20 mL) and then extracted with dichloromethane (200 mL and 4 \times 100 mL). The combined organic extracts were dried (Na₂SO₄) and concentrated under reduced pressure to yield **27** (1.94 g, 70% yield), which was recrystallized from *i*-PrOH (190 mL, recovery = 1.30 g, 67%). ¹H NMR (DMSO-*d*₆) δ 12.19 (s, 1 H), 9.83 (s, 1 H), 9.25–8.90 (bs, 1 H), 7.39 (dd, J = 8.5, 5.6 Hz, 2 H), 7.16 (app. t, J = 8.8 Hz, 2 H), 4.51 (d, J = 6.4 Hz, 2 H), 3.48 (s, 3 H), 2.56 (s, 3 H), 1.74 (s, 6 H). MS m/z 445 (M + H)⁺. HRMS calcd for C₂₀H₂₂O₄N₆F (M + H)⁺: 445.16302. Found: 445.16278. Melting point 216 °C.

Preparation of the Potassium salt of 27. A standard 0.5 N solution of KOH in H₂O (2.28 mL, 1.14 mmol) was added to a solution of **27** (510 mg, 1.14 mmol) in MeCN (20 mL), and the mixture was stirred at room temperature for 20 min. The resulting solution was frozen in a –78 °C bath and then freeze-dried to yield the desired potassium salt (553 mg, quant). This material was then

dissolved in refluxing EtOH (40 mL) and within a few minutes material crystallized out. The mixture was further refluxed for 10 min, cooled to rt, and left to stand for 4 h. The resulting crystals were filtered and dried yielding potassium 4-{[(4-fluorobenzyl)amino]carbonyl}-1-methyl-2-(1-methyl-1,3,4-oxadiazol-2-yl)carbonyl]amino}ethyl)-6-oxo-1,6-dihydropyrimidin-5-olate (401 mg, 72%). ^1H NMR (DMSO- d_6) δ 11.70–11.20 (bs, 1 H), 9.75 (s, 1 H), 7.33 (dd, J = 8.8, 5.8 Hz, 2 H), 7.12 (app. t, J = 8.8 Hz, 2 H), 4.44 (d, J = 5.8 Hz, 2 H), 3.40 (s, 3 H), 2.56 (s, 3 H), 1.70 (s, 6 H). Melting point 282 °C.

N-(4-Fluorobenzyl)-5-hydroxy-1-methyl-2-(1-methyl-1-[(5-methyl-4H-1,2,4-triazol-3-yl)carbonyl]amino}ethyl)-6-oxo-1,6-dihydropyrimidine-4-carboxamide (28). Following the procedure described for **21**, treatment of **35a** with 5-methyl-4H-1,2,4-triazole-3-carboxylic acid and purification by preparative RP-HPLC afforded the title compound in 72% yield. ^1H NMR (DMSO- d_6) δ 12.18 (bs, 1 H), 9.07 (bt, 1 H), 8.98 (bs, 1 H), 7.39 (dd, J = 8.5, 5.7 Hz, 2 H), 7.13 (t, J = 8.8 Hz, 2 H), 4.52 (d, J = 6.4 Hz, 2 H), 3.43 (s, 3 H), 2.48 (s, 3 H), 1.72 (s, 6 H). MS m/z 444 ($M + H$) $^+$. HRMS calcd for $C_{20}\text{H}_{23}\text{O}_4\text{NF}_7$ ($M + H$) $^+$: 444.17901. Found: 444.17925.

Acknowledgment. We thank Anna Alfieri and Francesca Naimo for plasma protein binding determination and for analytical chemistry, Silvia Pesci for NMR spectrometry, Vincenzo Pucci for accurate mass measurements, Peter Felock for the HIV-integrase enzymatic assays, William Schleif for the antiviral cell based assays, Massimiliano Fonsi and Marina Taliani for the microsome stability data, and Annalise Di Marco for the hepatocytes stability data.

Supporting Information Available: HPLC retention times are reported. This material is available free of charge via the Internet at <http://pubs.acs.org>.

References

- 1) 2006 Report on the Global AIDS Epidemic; UNAIDS: Geneva, Switzerland 2006.
- 2) Cervia, J. S.; Smith, M. A. Enfuvirtide (T20): a novel human immunodeficiency virus type 1 fusion inhibitor. *Clin. Infect. Dis.* **2003**, *37*, 1102–1106.
- 3) Dorr, P.; Westby, M.; Dobbs, S.; Griffin, P.; Irvine, B.; Macartney, M.; Mori, J.; Rickett, G.; Smith-Burchell, C.; Napier, C.; Webster, R.; Armour, D.; Price, D.; Stammen, B.; Wood, A.; Perros, M. Maraviroc (UK-427,857), a potent, orally bioavailable, and selective small-molecule inhibitor of chemokine receptor CCR5 with broad-spectrum anti-human immunodeficiency virus type 1 activity. *Antimicrob. Agents Chemother.* **2005**, *47*(21), 4721–4732.
- 4) Pommier, Y.; Johnson, A. A.; Marchand, C. Integrase inhibitors to treat HIV/AIDS. *Nat. Rev. Drug Discovery* **2005**, *4*, 236–248.
- 5) Zhuang, L.; Wai, J. S.; Embrey, M. W.; Fisher, T. E.; Egbertson, M. S.; Payne, L. S.; Guare, J. P.; Vacca, J. P.; Hazuda, D. J.; Felock, P. J.; Wolfe, A. L.; Stillmock, K. A.; Witmer, M. V.; Moyer, G.; Schleif, W. A.; Gabryelski, L. J.; Leonard, Y. M.; Linch, J. J.; Michelson, S. R.; Young, S. D. Design and synthesis of 8-hydroxy-[1,6]naphthyridines as novel inhibitors of HIV-1 integrase in vitro and in infected cells. *J. Med. Chem.* **2003**, *46*, 453–456.
- 6) Hazuda, D. J.; Young, S. D.; Guare, J. P.; Neville, A. J.; Gomez, R. P.; Wai, J. S.; Vacca, J. P.; Handt, L.; Motzel, S. L.; Klein, H. J.; Dornadula, G.; Danovich, R. M.; Witmer, M. V.; Wilson, K. A. A.; Tussey, L.; Schleif, W. A.; Gabryelski, L. S.; Jin, L.; Miller, M. D.; Casimiro, D. R.; Emini, E. A.; Shiver, J. W. Integrase inhibitors and cellular immunity suppress retroviral replication in rhesus macaques. *Science* **2004**, *305*, 528–532.
- 7) Ramirez, M. 10th European AIDS Conference 2006, Dublin, Ireland, 2006, Abstract LPBS1/6. Beatriz Grinsztejn, B.; Nguyen, B.; Katlama, C.; Gatell, J. M.; Lazzarin, A.; Vittecoq, D.; Gonzalez, C. J.; Chen, J.; Harvey, C. M.; Isaacs, R. D. Safety and efficacy of the HIV-1 integrase inhibitor raltegravir (MK-0518) in treatment-experienced patients with multidrug-resistant virus: a phase II randomised controlled trial. *Lancet* **2007**, *369*, 1261–1269.
- 8) For reviews on biology of HIV-1 integrase, see: (a) Esposito, D.; Craigie, R. HIV-Integrase Structure and Function. *Adv. Virus Res.* **1999**, *52*, 319–333. (b) Asante-Appiah, E.; Skalka, A. M. HIV-1 integrase: structural organization, conformational changes, and catalysis. *Adv. Virus Res.* **1999**, *12*, 2331–2338.
- 9) Hazuda, D. J.; Felock, P. J.; Witmer, M.; Wolfe, A.; Stillmock, K.; Grobler, J. A.; Espeseth, A.; Gabryelski, L.; Schleif, W.; Blau, C.; Miller, M. D. Inhibitors of strand transfer that prevent integration and inhibits HIV-1 replication in cells. *Science* **2000**, *287*, 646–650.
- 10) Summa, V.; Petrocchi, A.; Pace, P.; Matassa, V. G.; De Francesco, R.; Altamura, S.; Tomei, L.; Koch, U.; Neuner, P. Discovery of α,γ -diketo acids as potent selective and reversible inhibitors of hepatitis C virus NS5b RNA-dependent RNA polymerase. *J. Med. Chem.* **2004**, *47*, 14–17.
- 11) Grobler, J. A.; Stillmock, K.; Hu, B.; Witmer, M.; Felock, P.; Espeseth, A. S.; Wolfe, A.; Egbertson, M.; Bourgeois, M.; Melamed, J.; Wai, J. S.; Young, S.; Vacca, J.; Hazuda, D. J. Diketo acid inhibitor mechanism and HIV-1 integrase: implication for metal binding in the active site of phosphotransferase enzymes. *Proc. Natl. Acad. Sci. U.S.A.* **2002**, *99*, 6661–6666.
- 12) Summa, V.; Petrocchi, A.; Matassa, V. G.; Taliani, M.; Laufer, R.; De Francesco, R.; Altamura, S.; Pace, P. HCV NS5b RNA-dependent RNA polymerase inhibitors: from α,γ -diketoacids to 4,5-dihydroxypyrimidine- or 3-methyl-5-hydroxypyrimidinone carboxylic acids. Design and synthesis. *J. Med. Chem.* **2004**, *47*, 5336–5339.
- 13) Summa, V.; Petrocchi, A.; Matassa, V. G.; Gardelli, C.; Muraglia, E.; Rowley, M.; Gonzalez, Paz, O.; Laufer, R.; Monteagudo, E.; Pace, P. 4,5-Dihydroxypyrimidine Carboxamides and *N*-Alkyl-5-hydroxypyrimidinone Carboxamides Are Potent, Selective HIV-Integrase Inhibitors with Good Pharmacokinetic Profiles in Preclinical Species. *J. Med. Chem.* **2006**, *49*, 6646–6649.
- 14) Petrocchi, A.; Koch, U.; Matassa, V. G.; Pacini, B.; Stillmock, K. A.; Summa, V. From dihydroxypyrimidine carboxylic acids to carboxamide HIV-integrase inhibitors: SAR around the amide moiety. *Bioorg. Med. Chem. Lett.* **2007**, *17*, 350–353.
- 15) Pace, P.; Di Francesco, M. E.; Gardelli, C.; Harper, S.; Muraglia, E.; Nizi, E.; Orvieto, F.; Petrocchi, A.; Poma, M.; Rowley, M.; Scarpelli, R.; Laufer, R.; Gonzalez Paz, O.; Monteagudo, E.; Bonelli, F.; Hazuda, D.; Stillmock, K. A.; Summa, V. Dihydroxypyrimidine-4-carboxamides as novel potent and selective HIV-integrase inhibitors. *J. Med. Chem.* **2007**, *50*, 2225–2239.
- 16) Gardelli, C.; Nizi, E.; Muraglia, E.; Crescenzi, B.; Ferrara, M.; Orvieto, F.; Pace, P.; Pescatore, G.; Poma, M.; Rico Ferreira, M. R.; Scarpelli, R.; Homnick, C. F.; Ikemoto, N.; Alfieri, A.; Verdirame, M.; Bonelli, F.; Gonzalez Paz, O.; Monteagudo, E.; Taliani, M.; Pesci, S.; Laufer, R.; Felock, P.; Stillmock, K. A.; Hazuda, D.; Rowley, M.; Summa, V. Discovery and synthesis of HIV-integrase inhibitors: development of potent and orally bioavailable *N*-methyl pyrimidones. *J. Med. Chem.* **2007**, *50*, 4953–4975.
- 17) Raltegravir. www.aidsinfo.nih.gov/DrugsatNews/2007. Accessed 2007.
- 18) Guare, J. P.; Wai, J. S.; Gomez, R. P.; Anthony, N. J.; Jolly, S. M.; Cortes, A. R.; Vacca, J. P.; Felock, P. J.; Stillmock, K. A.; Schleif, W. A.; Moyer, G.; Gabryelski, L. J.; Jin, L.; Chen, I. W.; Hazuda, D. J.; and Young, S. D. A series of 5-amino-substituted 4-fluorobenzyl-8-hydroxy-[1,6]naphthyridine-7-carboxamide HIV-1 integrase inhibitors. *Bioorg. Med. Chem. Lett.* **2006**, *16*, 2900–2904.
- 19) Monteagudo, E.; Pesci, S.; Taliani, M.; Fiore, F.; Petrocchi, A.; Nizi, E.; Rowley, M.; Laufer, R.; Summa, V. Studies of metabolism and disposition of potent human immunodeficiency virus (HIV) integrase inhibitors using ^{19}F -NMR spectroscopy. *Xenobiotica* **2007**, *37*, 1000–1012.
- 20) Hazuda, D. J.; Anthony, N. J.; Gomez, R. P.; Jolly, S. M.; Wai, J. S.; Zhuang, L.; Fisher, T. E.; Embrey, M.; Guare, J. P., Jr.; Egbertson, M. S.; Vacca, J. P.; Huff, J. R.; Felock, P. J.; Witmer, M. V.; Stillmock, K. A.; Danovich, R.; Grobler, J.; Miller, M. D.; Espeseth, A. S.; Jin, L.; Chen, I. W.; Lin, J. H.; Kassahun, K.; Ellis, J. D.; Wong, B. K.; Xu, W.; Pearson, P. G.; Schleif, W. A.; Cortese, R.; Emini, E.; Summa, V.; Holloway, M. K.; and Young, S. D. A naphthyridine carboxamide provides evidence for discordant resistance between mechanistically identical inhibitors of HIV-1 integrase. *Proc. Natl. Acad. Sci. U.S.A.* **2004**, *101*, 11233–11238.
- 21) Pye, P. J.; Zhong, Y.-L.; Jones, G. O.; Reamer, R. A.; Houk, K. N.; Askin, D. A Polar Radical Pair Pathway to Assemble the Pyrimidinone Core of the HIV-Integrase Inhibitor Raltegravir Potassium. *Angew. Chem., Int. Ed.* **2008**, *47*, 4134–4136.
- 22) Pucci, V.; Bonelli, F. Development of a simple and reliable accurate mass liquid chromatography/electrospray ionization mass spectrometry method for high resolution accurate mass determinations of new drug entities on a triple quadrupole mass spectrometer. *Rapid Commun. Mass Spectrom.* **2007**, *21*, 3051–3059.
- 23) Org. Synth. Coll. **1943**, *2*, 29.